(4)

AD-A213 650

Final Technical Report
on
PHASE EQUILIBRIUM AND CRYSTAL GROWTH STUDIES ON $AgGaSe_2$ AND RELATED NONLINEAR OPTICAL MATERIALS

for the period
June 1, 1986 through December 31, 1988

submitted to
Office of Naval Research
800 North Quincey, Code 111D
Arlington, VA 22217-5000
ONR N00014-86-K-0343
CMR-89-6
Stanford SPO #3159

CENTER FOR MATERIALS RESEARCH

STANFORD UNIVERSITY • STANFORD, CALIFORNIA

(4)

The Board of Trustees of The
Leland Stanford Junior University
Center for Materials Research
Stanford, CA 94305-4045
Santa Clara, 12th Congressional District

Final Technical Report
on

PHASE EQUILIBRIUM AND CRYSTAL GROWTH STUDIES ON $AgGaSe_2$ AND RELATED NONLINEAR OPTICAL MATERIALS

for the period
June 1, 1986 through December 31, 1988

submitted to
Office of Naval Research
800 North Quincey, Code 111D
Arlington, VA 22217-5000
ONR N00014-86-K-0343
CMR-89-6
Stanford SPO #3159

Principal Investigator:

Robert S. Feigelson, Professor (Res.)
Center for Materials Research
Stanford, California 94305-4045
(415) 723-4007

September 1989

Unclassified

SECURITY CLASSIFICATION OF THIS PAGE

REPORT DOCUMENTATION PAGE

1a REPORT SECURITY CLASSIFICATION Unclassified	1b RESTRICTIVE MARKINGS
2a SECURITY CLASSIFICATION AUTHORITY	3 DISTRIBUTION/AVAILABILITY OF REPORT Approved for public release; distribution unlimited.
2b DECLASSIFICATION/DOWNGRADING SCHEDULE	
4 PERFORMING ORGANIZATION REPORT NUMBER(S) CMR-89-6	5 MONITORING ORGANIZATION REPORT NUMBER(S)
6a NAME OF PERFORMING ORGANIZATION The Board of Trustees of the Leland Stanford Jr. University 6b OFFICE SYMBOL (If applicable)	7a. NAME OF MONITORING ORGANIZATION
6c. ADDRESS (City, State, and ZIP Code) c/o Sponsored Projects Office, 40 Encina Hall Stanford University Stanford, CA 94305-	7b. ADDRESS (City, State, and ZIP Code)
8a. NAME OF FUNDING/SPONSORING ORGANIZATION Office of Naval Research 8b. OFFICE SYMBOL (If applicable)	9. PROCUREMENT INSTRUMENT IDENTIFICATION NUMBER N00014-86-K-0343
8c. ADDRESS (City, State, and ZIP Code) 800 N. Quincey Street, Code 1110 Arlington, VA 22217-5000	10. SOURCE OF FUNDING NUMBERS PROGRAM ELEMENT NO. / PROJECT NO. / TASK NO / WORK UNIT ACCESSION NO

11. TITLE (Include Security Classification)

Phase Equilibrium and Crystal Growth Studies on $AgGaSe_2$ and Related Nonlinear Optical Materials

12. PERSONAL AUTHOR(S)
Feigelson, Robert S. and Route, Roger K.

13a. TYPE OF REPORT	13b. TIME COVERED	14. DATE OF REPORT (Year, Month, Day)	15. PAGE COUNT
Final Technical	FROM 6/1/86 TO 12/31/88	September 1989	69

16. SUPPLEMENTARY NOTATION The view, opinions and/or finding contained in this report are those of the author(s) and should not be construed as an official Department of Navy position, policy, or decision unless so designated by other documentation.

17 COSATI CODES		
FIELD	GROUP	SUB-GROUP

18. SUBJECT TERMS (Continue on reverse if necessary and identify by block number)
Silver selenogallate, $AgGaSe_2$, nonlinear optical materials, infrared materials, optical defects

19. ABSTRACT (Continue on reverse if necessary and identify by block number)

This report summarizes a 31 month research program carried out at the Center for Materials Research, Stanford University. The principal objectives were 1) to improve the crystal growth technology for $AgGaSe_2$ to facilitate the growth and yield of useful size nonlinear optical elements; 2) to gain an increased understanding of the optical scattering precipitates that form in melt-grown crystals; 3) to determine the cause of residual optical absorption remaining after post-growth heat-treatment; 4) to refine the heat-treatment procedure so as to eliminate residual optical absorption; and 5) to elucidate the chemistry and thermodynamics of the heat-treatment procedure. The first four objectives were met successfully and are described fully. The final objective, the topic of a graduate student dissertation research project is still ongoing, and progress to date is described in detail.

20 DISTRIBUTION/AVAILABILITY OF ABSTRACT	21 ABSTRACT SECURITY CLASSIFICATION
☐ UNCLASSIFIED/UNLIMITED ☐ SAME AS RPT. ☐ DTIC USERS	Unclassified
22a. NAME OF RESPONSIBLE INDIVIDUAL	22b. TELEPHONE (Include Area Code) / 22c. OFFICE SYMBOL

DD FORM 1473, 84 MAR 83 APR edition may be used until exhausted. All other editions are obsolete

SECURITY CLASSIFICATION OF THIS PAGE

☆ U.S. Government Printing Office: 1986—607-044

TABLE OF CONTENTS

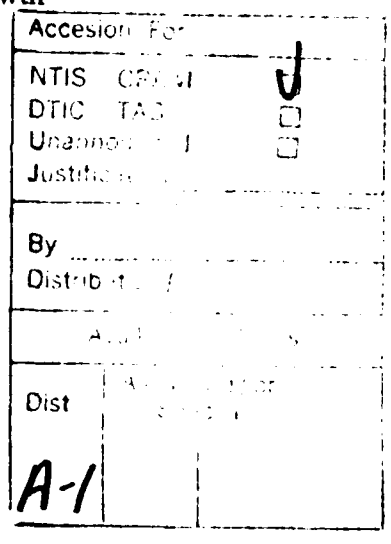

ABSTRACT

This report summarizes a 31 month research program carried out at the Center for Materials Research, Stanford University. The principal objectives were 1) to improve the crystal growth technology for $AgGaSe_2$ to facilitate the growth and yield of useful size nonlinear optical elements; 2) to gain an increased understanding of the optical scattering precipitates that form in melt-grown crystals; 3) to determine the cause of residual optical absorption remaining after post-growth heat-treatment; 4) to refine the heat-treatment procedure so as to eliminate residual optical absorption; and 5) to elucidate the chemistry and thermodynamics of the heat-treatment procedure. The first four objectives were successfully accomplished and are described fully. The final objective, the topic of a graduate student dissertation research project is ongoing, and progress to date is summarized.

I. INTRODUCTION

A. OBJECTIVES

This is the final technical report summarizing a research program, originally designed for 36 months, on "Phase Equilibrium and Crystal Growth Studies on $AgGaSe_2$ and Related Non-linear Optical Materials, ONR Contract No. N00014-86-K-0343. The program began at Stanford University on June 1, 1986 and terminated on December 31, 1988.

Our main objective was to gain an in-depth understanding of the thermodynamics, solid-state kinetics, and growth properties in the Ag-Ga-Se system so that large high optical quality crystals of $AgGaSe_2$ could be reproducibly grown to satisfy the very strong demand for this material that has arisen over the past few years.

The initial few months of the program were devoted to scaling up our crystal growth systems to produce 37 mm diameter boules from which longer, more efficient mixing and SHG crystals could be cut. After that was accomplished, we focused mainly on seeking an increased understanding of the optical defects that form in $AgGaSe_2$ and the chemical thermodynamics of the heat-treatment procedures that are used to eliminate them. Based on this work, we made modifications to the crystal growth process to test the applicability of this new data in improving the quality of the crystals produced.

In October, 1987 we were requested by ONR to reduce the length of this program from the originally proposed 36 months to 29 months in order to coincide with normal fiscal year funding cycles. A major budget reduction was also requested, from the $522.4 K originally proposed to $347.4 K, in order to match limited funding resources. A reduction in the scope of the proposed program was, therefore, necessary but many of the essential aspects of the program were preserved.

B. APPROACH

The research carried out during this program was divided into five discrete elements: 1) scale up to the growth of 37 mm dia. boules from which multicentimeter optical crystals could be cut, 2) elucidating the nature of the residual absorption/scatter losses that remained after heat-treatment and varied from one crystal to the next, 3) growth of novel shapes to enhance cutting yields and increase the opportunities for efficient commercialization, 4) identifying the exact chemical interdiffusion process(es) occurring during heat-treatment, and 5) evaluating the effects on crystalline and optical properties of melt stirring by a newly developed technique known as coupled vibrational stirring (CVS).

The last two studies are still in progress at this writing as a graduate student dissertation research project. Research in the first three categories has been summarized in detail in manuscript form for submission to relevant technical journals. These form the basis for the first three sections under research results. The ongoing studies on chemical interdiffusion and melt stirring form the basis of the final two sections.

II. RESEARCH RESULTS

A. GROWTH OF SILVER SELENOGALLATE CRYSTALS BY THE VERTICAL BRIDGMAN METHOD

1. Background

Silver selenogallate ($AgGaSe_2$) is a I-III-IV_2 compound that crystallizes in the chalcopyrite structure. It was shown more than 10 years ago that this materials has unique nonlinear infrared optical properties[1-4] including high nonlinear coefficients, and the ability to be phase matched through a relatively large portion of its transparency range. $AgGaSe_2$ is transparent from 0.73 to 17 μm. Free-carrier absorption is negligible since the material is semi-insulating. Although a few reports of its use in nonlinear optical applications have appeared in the literature throughout the past 15 years,[5-6] its full potential was never realized due to challenging problems in crystal growth and control of optical quality.

$AgGaSe_2$ is reactive with O_2 and H_2O and somewhat volatile at its melting point of 856°C. Hence, it must be grown in sealed quartz growth ampoules. The chalcopyrite structure, space group $\bar{4}2m$, is based upon the zinc blend structure of the III-V group but has lower symmetry due to alternate ordering in the cation sublattice. The unit cell is tetragonal, as shown in Fig. 1, and mechanical and optical properties are different in directions parallel to and normal to the optic, or c-axis.

Initial crystal growth experiments on this material revealed a number of problem areas including, 1) crystal and ampoule cracking, 2) bands of inclusions, 3) compositional grading, 4) twins, and 5) poor optical quality [7,8] The crystals had a milky appearance due to a high density of micrometer-size scattering centers.[4,5,8-10]

One of the most important discoveries leading to the successful growth of this material was that by Iseler[6] who showed that $AgGaSe_2$ has anomalous thermal expansion behavior and actually expands along the c-axis as it cools. These expansion curves are plotted in Fig. 2. The second important advance was in developing a heat-treatment procedure that was effective in eliminating the scattering centers in as-grown crystals. This was first shown by Matthes et al.[11] for $AgGaS_2$ and by Route et al.[12] for $AgGaSe_2$. The current highly successful crystal growth technology is based on the early work in these two areas.

2. Materials Synthesis

$AgGaSe_2$ melts congruently, and details of the phase equilibria in the Ag_2Se-Ga_2Se_3 binary join are known[12-14] The compound is typically made by reaction of high-purity, 99.999% or better, starting materials in elemental form in a separate procedure. In our work we have studied compositions close to stoichiometric. Chemical reaction is carried out in evacuated and sealed fused-quartz ampoules that are internally coated with carbon by pyrolysis of an organic vapor. Elemental selenium has a relatively low vapor pressure, so chemical reaction by direct fusion can be used. A polycrystalline charge is obtained from the synthesis that is cracked and shows evidence of compositional variations. This is now known to be unavoidable. The material is then finely broken to achieve some degree of homogenization before it is used as a charge for crystal growth.

3. Bridgman-Stockbarger Crystal Growth

Crystals are grown by the standard Bridgman-Stockbarger method in a 2 1/2 in. internal diameter (ID) resistance-wound tubular two-zone furnace. Temperature gradients at the growth interface are nominally 18°C/cm, measured in the open bore. With the growth ampoule present, this is reduced somewhat to 14° C/cm.

There are two essential features to the successful growth $AgGaSe_2$ in sealed quartz ampoules. First, since the crystals are known to expand along their optic [001] axis during cooling, they must be seeded so that the c-axis is close to the axis of the growth ampoule. (Crystals that nucleate spontaneously typically end up with the c-axis tipped far enough over from the ampoule axis that a net transverse expansion occurs during cooling, with disastrous results.) Second, since c-axis boules expand along their lengths during cooling, the ampoules must be designed so that mechanical restrictions along their lengths cannot occur. We have solved this problem by designing our fused-quartz growth ampoules with a continuous 1 1/2° taper in both the seed pocket and the main body.

The flare-out region is usually designed with a 20° internal half-angle. Commercial fused-quartz tubing cannot be selected and worked so as to introduce the appropriate taper while maintaining a perfectly round internal cross section. To produce growth ampoules with the desired interior dimensions we have developed a vacuum-forming method by which slightly oversized fused-quartz tubing can be collapsed upon a precision-machined graphite mandrel. Replication of the mandrel surface is exact, and the internal finish is smooth except where machining imperfections on the mandrel surface have occurred. The growth ampoules used in this work were 28 mm ID with a 6 mm diameter by 15 mm long

seed pocket, and 37 mm ID with an 8 mm diameter by 25 mm long seed pocket. A carbon mandrel and a vacuum-formed ampoule are shown in Fig. 3. Prior to use, the growth ampoules are internally coated with carbon by pyrolysis of an organic vapor.

Accurately oriented c-axis seeds are hand-fitted to the growth ampoules by a taper grinding method. A few mils' clearance is allowed for transverse thermal expansion during heat-up. Boules are designed to be 10 to 12 cm in length, which requires crushed polycrystalline charges of up to 520 g for the 37 mm diameter boules. Prior to sealing, the charged growth ampoules are evacuated to pressures less than 10-5 Torr and then back-filled with 0.5 atmosphere of argon gas purified by passing it through a titanium sponge reactor at 750°C. Seed attachment is controlled by monitoring a platinum-rhodium thermocouple held against the side of the seed pocket by spring tension. The furnace configuration is shown in Fig. 4. Seeding temperatures, determined empirically, were found to be quite close to the congruent melting point. Crystal growth is then carried out at approximately 15 mm/day. When solidification is complete, the crystals are cooled in the shallow-gradient, lower zone of the furnace at a rate of 50°C/h.

Properly seeded boules are found to be loose in their ampoules after growth. Occasionally, secondary nucleation on the surfaces is observed. This is thought to be related to failure of the carbon coating. Polycrystalline boules are always seriously cracked due to thermal expansion anisotropy. Minor surface spalling is also occasionally found around localized surface imperfections. In most cases, however, boules remained single and are of excellent structural quality. Refinement of the technique has allowed us to grow crystals with very few surface voids. Twins, present in almost all early work, do not occur as long as mechanical interaction with the growth ampoules is carefully prevented. A 28 mm AgGaSe2 boule free of structural imperfections is shown in Fig. 5. Compositional variations are always observed independent of the charge composition. A thin band of black material always found on the top of these boules was determined by dispersive analysis to be Ag and Sc rich.

4. Optical Defects

The as-grown crystals of $AgGaSe_2$ were always found to have a milky appearance in thin section or when viewed with a commercial infrared image converter. Microscopic examination of $AgGaSe_2$ in both reflected and transmitted light reveals micrometer-wide linear defects, approximately 100 μm long, oriented along the [100] and [010] directions (Fig. 6). Extensive metallographic preparation and optical microscopic

evaluation were carried out in our laboratory on $AgGaSe_2$ and the closely-related material $AgGaS_2$ which has similar defects. The defects were found to consist of precipitates surrounded by localized strain fields.[15] In Fig. 7 we show localized strain fields surrounding precipitates in $AgGaS_2$. Careful etching and ion-beam milling studies showed that the precipitates in $AgGaSe_2$ are actually 100 μm rectangular platelets lying on the [100] and [010] planes, Fig. 8. The defects are slightly richer than the matrix in both Ga and Se. A corresponding situation is true for the case of $AgGaS_2$, Fig. 9.

5. Phase Equilibrium Studies

The precipitates and their surrounding strain fields can be removed from $AgGaSe_2$ by quenching from temperatures above 650°C, and by heat-treatment in the presence of Ag_2Se[12] or excess stoichiometric $AgGaSe_2$ powder.[16,17] To account for this effect, one must understand the thermodynamic phase equilibria along the Ag_2Se-Ge_2Se_3 pseudobinary join. Differential thermal analysis (DTA) studies on compositions along this join in the vicinity of the stoichiometric composition have been carried out here and elsewhere[12-14] to elucidate the nature of the phase equilibria.

The most detailed study of the phase equilibria in the Ag-Ga-Se system was by J. C. Mikkelsen, Jr. in his determination of the phase equilibria along the Ag_2Se-Ga_2Se_3 pseudobinary join[14], Fig. 10a. He reported a measurable solubility of excess Ga_2Se_3 in $AgGaSe_2$ in the range of several mole percent at elevated temperatures. Below 832°C, however, the solubility is retrograde. While he found no direct evidence of the congruently melting composition deviating from stoichiometry by DTA analysis, solidification studies showed that stoichiometric melts solidified with an excess of Ga_2Se_3 in the first to freeze sections and that during cooling the excess Ga_2Se_3 comes out of solution as a precipitate of nominal composition $AgGa_7Se_{11}$. Brandt and Kramer[18] found a very similar situation in their determination of the phase equilibria along the Ag_2S-Ga_2S_3 pseudobinary join.

In the Bridgman growth of large boules, we have found very consistent behavior. Stoichiometric melts always reject silver-rich material during growth, implying the material solidifies with excess Ga_2Se_3 in solution. Precipitates are always found after cooling. Electron beam microprobe analysis consistently has shown the precipitates to be rich in Ga and Se, but could not identify their exact chemical composition. No attempt was made to isolate x-ray diffraction patterns of the precipitate phase from the matrix phase due to the lack of sensitivity of the method.

Based on our results, we proposed the nonstoichiometric congruency modification to the phase diagram as shown in Fig. 10b.[12] The phase equilibria thus modified accounts for much of the phenomena observed during growth of $AgGaSe_2$. All crystals grown from near-stoichiometric melts contain excess Ga_2Se_2 which precipitates during cooling as an intermediate phase (presumably $AgGa_7Se_{11}$) due to retrograde solubility. This model is consistent with our electron microprobe studies of precipitates in $AgGaSe_2$ as well as with the tendency of all $AgGaSe_2$ boules to reject silver-rich material as they grow from stoichiometric melts.

The above model suggests that optically clear material, free of precipitates, might be grown from Ag_2Se-rich solutions in which the liquidus temperature is below the point at which the existence region departs from stoichiometry. In the closely related sulfide system, a series of growth experiments was carried out from Ag_2S-rich solutions, as shown in Fig. 11, to demonstrate this effect. For solutions of greater than 65 mole % Ag_2S, in which the liquidus temperature is in the neighborhood of 960°C, optically clear crystals were obtained. The method is totally impracticable for the controlled growth of large high quality crystals, however, due to the obvious difficulties in seeding and the need to reject large amounts of material from the growing crystal interface. The growth of high quality but cloudy crystals from congruent melts followed by a heat-treatment procedure turns out to be a far more effective approach.

6. Heat-Treatment Procedures

Oriented slabs of $AgGaSe_2$ are first cut from as-grown boules. These are then heat treated in a sealed quartz ampoule for 14 to 21 days at 800°C, according to the procedure shown in Fig. 12, using approximately 1.5 wt. % excess Ag_2Se. Physical contact between the Ag_2Se and the bulk $AgGaSe_2$ crystal seems to be necessary for optimum results. Even without it, however, Ga_2Se or (2Ga + 3/2 Se_2) volatilizes from the surface of the bulk $AgGaSe_2$ crystal and reacts with the Ag_2Se_3 to produce $AgGaSe_2$ + liquid (L). In either case, chemical interdiffusion removes excess Ga_2Se_3 from the bulk crystal, allowing it to homogenize to a stoichiometric composition on the left-hand boundary of the existence region, from which precipitation due to retrograde solubility does not occur. In Fig. 13, we show an optical photograph of a tungsten filament imaged through a 1 cm thick $AgGaSe_2$ crystal with an IR converter. In Fig. 13a, the filament was imaged through an as-grown crystal, and in Fig. 13b the filament was imaged through a

heat-treated crystal. Optical clarity in completely heat-treated crystals is excellent and no scattering is detectable to the eye.

7. Optical Crystals

Using the crystal growth and postgrowth heat-treatment procedures described, we have successfully produced near-theoretically transparent, oriented crystals approximately 1 cm in cross section. The lengths vary slightly depending on the propagation direction, which is determined by the phase-matching conditions. For most experiments it has been possible to fabricate $AgGaSe_2$ crystals in excess of 22 mm long from 28 mm diameter boules and $AgGaSe_2$ crystals in excess of 35 mm long from 37 diameter boules. Most crystals are oriented with the propagation direction between 45° and 90° to the boule axis. Because of the anomalous thermal expansion problem, for all useful phase-matched applications, we are prevented from growing the crystals sufficiently close to the propagation direction to harvest substantially longer crystals. To obtain longer interaction lengths, crystals of larger diameter must be grown.

8. Recent Nonlinear Optical Results

With the high optical quality, twin-free crystals of $AgGaSe_2$ described, significant advances in nonlinear IR optical technology have been made. Principal among these are the demonstration of optical parametric oscillation in $AgGaSe_2$[19] and efficient second-harmonic conversion of the carbon dioxide laser.[20,21] Details of these experiments are included in Table II.

The current limitation of the material is its relatively moderate threshold for surface damage, which is in the 10 to 15 MW/cm^2 range, and broad band residual absorption, or scattering, in the 0.5- 2.5% cm-1 range which varies from one crystal to the next. Preliminary experimentation with various anti-reflection surface coatings has indicated that damage threshold values may be raised by a factor of 2 or more, and consequently, higher conversion efficiencies should be possible. Recent studies revealing residual precipitates after heat-treatment indicate that the current procedure may not be yielding optimum results in all cases. This is discussed more fully in section B.

9. Summary of Results

The practical problems associated with the growth of high optical quality, twin-free crystals of $AgGaSe_2$ have been resolved. Near-theoretically transparent crystals

1 cm in cross section and in lengths exceeding 35 mm, have been produced. With these, useful and practical solid-state nonlinear infrared optical devices have been realized.

TABLE I

RESULTS OF EXPERIMENTS ON $AgGaSe_2$

		Reference
Parametric oscillation	pump wavelength: 2.05 μm output wavelengths: 2.65-9.02μm	19
Second-harmonic generation	pump wavelength: 10.25 μm output wavelength: 5.13 μm energy conversion efficiency: 14%	20
Second-harmonic generation	pump wavelength: 10.6 μm output wavelength: 5.3 μm harmonic conversion efficiency: 18.7%	21
Damage	Surface damage thresholds have been measured at a number of wavelengths. For 20-50 ns pulses they are typically 13 MW/cm2. Bulk damage thresholds are at least one order of magnitude higher.	19-21

B. IMPROVEMENTS IN THE OPTICAL QUALITY OF $AgGaSe_2$ CRYSTALS

1. Introduction

Even with relatively successful heat-treatment procedures to eliminate scattering defects, residual scattering defects do occur, and residual optical losses in the few % cm-1 range and varying from one crystal to the next, are found. The purpose of this study was to take a more detailed look at the nature of the scattering in $AgGaSe_2$ using improved optical characterization techniques, and to correlate this data, and variations in the heat-treatment procedures used, with the known phase equilibria in the Ag_2Se-Ga_2Se_3 pseudobinary system.

2. Experimental Procedures

a. Heat-Treatment

Oriented slabs and crystals of as-grown $AgGaSe_2$ containing precipitates in varying concentrations were heat treated in evacuated and sealed fused quartz ampoules according to the procedure shown in Fig. 12 for 14 to 21 days at temperatures near 800°C. This procedure was essentially the same as that reported by us previously.[12,22] Excess Ag_2Se was varied in the range 0-2 wt %. In a few experiments, contact between the $AgGaSe_2$ crystals and the excess Ag_2Se occurred only through the vapor phase, but in most, direct physical contact was ensured by placing the $AgGaSe_2$ crystals on top of the excess Ag_2Se. Heating and cooling rates of 50° C/hr were used to minimize thermal shock.

b. Evaluation

Evaluation of optical scattering due to the presence of precipitates was carried out by several methods: low power evaluation using a commercial IR image converter in a transmitted light mode; high power IR microscopic examination in a transmitted light mode; visible high power optical microscopic evaluation of thin sections which are reasonably transparent; spectrophotometer transmission measurements throughout the transparency range; and silicon vidicon video imaging of scattered light using dark field and bright field illumination.

3. Results

After heat-treatment, previously polished $AgGaSe_2$ surfaces were found to be roughened. Repolishing was, therefore, necessary before optical evaluation could be carried out. Whether or not physical contact occurred, chemical reaction with the excess Ag_2Se occurred, causing the formation of a liquid phase in contact with the excess Ag_2Se. Minor amounts of fracturing were found in the contact region whenever physical contact between the $AgGaSe_2$ crystals and the liquid phase occurred. To minimize the losses due to fracturing, $AgGaSe_2$ crystals were stood vertically so that only their smaller end was in physical contact with the excess Ag_2Se.

Weight measurements made before and after heat-treatment in the case of vapor phase communication only, showed a net transport of material from the $AgGaSe_2$ crystals to the excess Ag_2Se + liquid (L). X-ray diffraction analysis of the solidified Ag_2Se + L, consistently reveals diffraction peaks corresponding to the chalcopyrite structure of $AgGaSe_2$. It is apparent that both gallium and selenium transport through the vapor phase during the heat-treatment procedure, but the specific chemical species they form and the exact transport mechanism are unknown.

a. Single Heat-Treatment Cycle

Physical contact between the Ag_2Se and the bulk $AgGaSe_2$ crystal was found to be necessary for optimum results and 1.5 wt % excess Ag_2Se was found to be sufficient to achieve good optical clarity. $AgGaSe_2$ crystals heat treated at 800° C for 14-21 days with 1.5 wt % excess Ag_2Se in contact were found to be essentially clear of visible scattering under transmitted illumination detected with a commercial low power IR image converter. In Fig. 13, we showed an optical photograph of a tungsten filament imaged through a 1 cm thick $AgGaSe_2$ crystal with an IR converter. In Fig. 13a, the filament was imaged through an as-grown crystal, and in Fig. 13b the filament was imaged through a singly heat-treated crystal. Optical clarity in heat-treated crystals is excellent and no scattering is detectable by this method.

Under high power IR microscopy, remnant microscopic defects in the 10 mm size range are observed, usually in densities substantially lower than the density of the precipitates in as-grown crystals. These sometimes appear as negative crystals (internally faceted voids), Fig. 14. Usually, however, they appear as clusters of roughly spherical shapes when viewed in transmission under high power IR microscopy or in thin section under high power optical microscopy, Fig. 15a. Because of their small size and low

density they are difficult to study using energy dispersive or microprobe methods. Their exact chemical composition is currently unknown, although both of these analytical methods consistently show enrichment of gallium at the defect sites. Often, the clusters are similar in shape to the original precipitates, Fig. 15b. This suggested that they could be caused by incomplete chemical reaction during heat-treatment. Changing the duration of heat-treatment and the quantity of Ag_2Se used did not produce a noticeable change in the size and density of these defects beyond the normal variation seen from one crystal to the next, however.

The microscopic defects remaining after heat-treatment do not significantly affect optical transparency. Spectrophotometric transmission analysis yields near-theoretical values throughout a large portion of the transparency range. Nor does their presence seriously influence efficient non-resonant second harmonic generation of the CO_2 laser.[20,21] However, in resonant intracavity applications such as tunable optical parametric oscillators,[19] small absorption and scattering losses can have more serious consequences. Careful power balance measurements on many crystals from a number of different $AgGaSe_2$ boules have always yielded losses in the 0.5-2.5 % cm-1 range,[23] varying from one crystal to the next. Only weak correlations could be made between power loss measurements and the size and density of the residual defects shown in Figs. 5 and 6.

b. Improved Imaging Techniques

Recently, we have begun using a scattered light technique to observe scattering defects in heat-treated AgGaSe2 crystals.[24] The optical setup is illustrated in Fig. 16, and it relies on the near-IR sensitivity of standard video cameras with either silicon vidicon or CCD array detectors, and the high resolution processing of readily available video equipment. The method has so far been used only on a macroscopic scale to observe optical scattering in cm+ size specimens. In Fig. 17, we show a video image of a 3 cm long $AgGaSe_2$ crystal in dark field illumination that clearly reveals the presence of light scattering centers in the core region, and clear regions under what were the exposed surfaces of the parent slab during heat-treatment. This behavior is typical of an incomplete vapor phase chemical interdiffusion reaction. Virtually all $AgGaSe_2$ crystals studied displayed this effect in varying degrees if they had been subjected to a single heat-treatment procedure, and this effect is felt to be responsible for the variability in optical quality from one heat treated crystal to the next.

c. Secondary Heat-Treatment

Repeating the heat-treatment procedure described above with the following two minor modifications has been found effective in removing most of the remaining light scattering defects from the core regions of slabs and fabricated crystals. First, lesser amounts of Ag_2Se, on the order of 0.2 wt % have been found sufficient. Second, physical contact during heat-treatment does not seem to be necessary. This has the great benefit of causing only minor surface roughening so that repolishing is fairly simple. In Fig. 18 we show a video image of two $AgGaSe_2$ crystals from the same boule, one that was subjected to secondary heat-treatment and one that was not. Very little evidence of residual scattering defects can be seen in the doubly heat-treated crystal. Under high power IR microscopic examination, the microscopic defects seen after a single heat-treatment cycle cannot be detected.

Careful bright field illumination in the same optical setup has also been found to reveal the presence of residual absorption by localized scattering. Figure 19 compares $AgGaSe_2$ crystals from the same boule treated by single and double heat-treatment procedures. Under bright field illumination, absorption by scattering from the central core region is not as evident as under dark field illumination but the boundaries between the clear areas and those containing scattering centers are still quite distinct.

4. Discussion

The distribution of scattering defects in the core region of singly heat treated $AgGaSe_2$ clearly shows that the chemical interdiffusion reaction is incomplete. Using increased amounts of Ag_2Se and increasing the duration of the initial heat-treatment process have not produced the same results as opening the ampoule, removing the solidified Ag2Se-rich material, adding additional Ag_2Se, and reheat-treating. Since there are two species in the Ag-Ga-Se system that can transport through the vapor phase (Ga and Se), the condensed phase, Ag_2Se-Ga_2Se_3 phase diagram is not adequate to predict the subtle behavior observed in the melt growth of $AgGaSe_2$.

To obtain a quantitative measure of optical loss due to combined absorption and scatter, power balance measurements are desirable. Spectrophotemetric transmission measurements, Fig. 20, are not sensitive enough to resolve the differences between singly and doubly heat-treated crystals. However, power balance measurements are difficult to make on doubly heat-treated $AgGaSe_2$ crystals due to their low losses. Spectrally resolved, integrating sphere measurements of scattered light, and laser calorimetric

measurements of true absorption are complicated and time consuming. These are currently planned, but a more immediate determination of relative optical quality was desired. Apeturing of the video camera with constant dark field specimen illumination was used to obtain a rough measure of relative light scattering between singly heat-treated control crystals and doubly heat-treated crystals. A minimum of two aperture stops improvement was noted. Because no gradation in scattering intensity was detected in the core regions of the doubly heat-treated crystals, and because considerable scattering from the surfaces and iris was seen, it is suspected that the true reduction in scatter may exceed two aperture stops.

5. Summary of Results

Gallium selenide-rich precipitates in crystals of AgGaSe2 grown from near-stoichiometric melts have been eliminated by chemical interdiffusion in a double heat-treatment procedure. Optical absorption and scatter from doubly heat-treated crystals are barely detectable using conventional measurement methods. Visualization using the near-IR sensitivity of current video equipment was shown to be a valuable adjunct in the evaluation of IR-transparent semiconducting compounds.

C. IMPROVED YIELD OF BRIDGMAN-GROWN $AgGaSe_2$ CRYSTALS USING SHAPED CRUCIBLES

1. Introduction

Careful engineering over the last few years[22] has made possible the successful growth of $AgGaSe_2$ crystals by the standard Bridgman technique using growth ampoules with circular cross-sections. Since $AgGaSe_2$ crystals for specific device applications must be cut at various angles to the optic axis (55° for doublers and 48° for OPO's), the yield of crystals per boule is an important consideration. This study addressed the question of whether crystals could be grown from square cross-section growth ampoules with controlled crystallographic orientation.

2. Experimental Methods

a. Bridgman-Stockbarger Crystal Growth

Crystals of $AgGaSe_2$ are typically grown by the standard Bridgman-Stockbarger method in a 2 1/2 in. internal diameter (ID) resistance-wound tubular two-zone furnace, as shown in Fig. 4. Temperature gradients in the empty furnace at the melting point are nominally 18°C/cm. With the growth ampoule present, this is reduced to 14° C/cm.

There are two essential features to the successful growth $AgGaSe_2$ in sealed quartz ampoules. First, since the crystals expand along the optic (c)-axis during cooling, they must be seeded so that can expand freely into the free space of the growth ampoule, i.e. the c-axis must be aligned closely with the ampoule axis. (Crystals that nucleate spontaneously typically end up with the c-axis tipped far enough over from the ampoule axis such that a net transverse expansion occurs during cooling, with disastrous results.) Second, the ampoules must be produced without internal diameter variations which can restrict free expansion of the crystals. We have solved this problem by designing our fused-quartz growth ampoules with a continuous 1 1/2° taper in both the seed pocket and the main body.

The flare-out region is usually designed with a 20° internal half-angle. Commercial fused-quartz tubing cannot be selected and hand worked to produce a uniform predetermined taper with a perfect conical internal cross-section. To produce growth ampoules with the desired interior dimensions we have developed a vacuum-forming method by which slightly oversized fused-quartz tubing can be collapsed upon a precision-machined graphite mandrel. Replication of the mandrel surface is exact. The growth ampoules used in this work were of two types: 1) circular cross-sections of 37 mm ID

with an 8 mm diameter, 25 mm long seed pocket, and 2) square cross-sections of 28-31 mm with 7.5 -8 mm, 25 mm long seed pockets. Figure 21 illustrates the basic fabrication technique which uses a standard glass working lathe equipped with a vacuum swivel. For best results, the quartz tubing is handworked until it is slightly oversize, and in a single pass using a cross-fire torch, the tubing is collapsed upon the carbon mandrel. Fabrication of round cross-sections is considerably easier than square cross-sections which require a little more effort. Figures 22 and 23 show examples of both round and square carbon mandrels and the fabricated vacuum-formed fused quartz ampoules produced from them. Prior to use, the growth ampoules are internally coated with carbon by pyrolysis of an organic vapor.

Accurately oriented c-axis seeds were hand-fitted to the growth ampoules by a taper grinding method. A few mils' clearance was allowed for transverse thermal expansion during heat-up. For square cross-section boules, the side faces of the seeds were oriented normal to the {110} plane which is the plane in which light propagates during Type I phase-matched nonlinear interactions. Boules were designed to be 10 to 12 cm in length, which required crushed polycrystalline charges of approximately 500 g. Prior to sealing, the charged growth ampoules were evacuated to pressures less than 10-5 Torr and then back-filled with 0.5 atmosphere of argon gas purified by passing it through a titanium sponge reactor at 750°C. Seed attachment was controlled by monitoring a platinum-rhodium thermocouple held against the side of the seed pocket by spring tension, as shown in Fig. 4. Seeding temperatures, determined empirically, were found to be quite close to the congruent melting temperature. Crystal growth rates were 8-15 mm/day. When solidification was complete, the crystals were cooled in the shallow-gradient, lower zone of the furnace at a rate of 50°C/h. After growth, the boules were lightly sanded and inspected with an IR image converter for gross flaws. They were cut into two 1 cm+ thick slabs having {110} surfaces using a diamond saw and then heat-treated to eliminate optical defects.[12,24]

3. Results

Properly seeded boules were found to be loose in their ampoules after growth. Occasionally, polycrystallinity at the surfaces was observed. This is thought to be related to failure of the carbon coating. (Polycrystalline boules always crack seriously due to the thermal expansion anisotropy.) Minor surface spalling was also occasionally found around localized surface imperfections. In most cases, however, boules remained single

and were of excellent structural quality, Fig. 24. Twins, present in almost all early work, do not occur as long as mechanical interaction with the growth ampoule is carefully prevented. In this regard, the use of a pyrolytic carbon layer on the interior of the crucible seems to be important. A control crystal grown in a round vacuum-formed ampoule without an internal carbon coating was found to contain a number of planar defects assumed to be {112} mechanical twins. Compositional variations were always observed independent of charge composition, which in our case varied around the stoichiometric composition. A thin band of black material was always found on the top of these boules and was found, by dispersive analysis, to be Ag and Se rich, and has been assumed to consist of a eutectic mixture of Ag_9GaSe_6 and $AgGaSe_2$, consistent with the known phase equilibria in the system.

Minor cracking often extended downward from the Ag_2Se-rich region at the tops of the boules. This was thought to be due to differential thermal expansion during cooling. Growth closer to the congruent composition which contains 0.5 mole% excess Ga_2Se_3 should minimize this effect, but may also lead to a greater density of scattering centers. Currently, the two-step 800° C heat-treatment process described in section B is used to eliminate scattering defects in $AgGaSe_2$[16] caused by retrograde solubility. The first of the two steps is done prior to diamond sawing for stress relief purposes to minimize propagation of the Ag_2Se-related cracks at the top of the boule.

4. Discussion

Table II illustrates the yields possible from a circular cross-section boule compared to a square one for finished slabs of equivalent size. Assuming 1 mm kerf losses, approximately 63-64% of a circular cross-section boule is harvestable in slab form compared to 95% from a square cross-section boule. Scrap $AgGaSe_2$, worth approximately $1/gram, representing 26% and 30% of total mass as reclaimable material from a 30 mm dia and a 45 mm dia boule respectively, can be regrown. The additional costs of cleaning and regrowing this recoverable material in less expensive circular cross-section ampoules must be balanced against the use of fewer but more expensive square cross-section ampoules.

Reuse of ampoules has been possible as long as chemical reactions between the melt and the ampoule walls are strictly prevented by the use of a dense, well-adhering pyrolytic carbon coating. Once-grown, near-stoichiometric $AgGaSe_2$ does not interact at all with unprotected fused quartz; nor does Ag_2Se. During heat-treatment, direct contact

with uncoated fused quartz is routinely used. However, during charge synthesis we have not rigorously excluded surface oxides and other contaminants from the high purity elemental starting materials. The charges likely contain dispersed oxide contaminants which would be much more likely to react with unprotected fused quartz at growth temperatures. On occasions when failure of the pyrolytic carbon has occurred, definite indications of chemical reaction with the underlying quartz were observed, and during attempted reuse of these crucibles secondary breakdown was occasionally seen.

The essential feature of this work is that even with materials such as $AgGaSe_2$ and $AgGaS_2$ which display anomolous thermal expansion during cooling, it is possible to grow defect-free single crystals in fused quartz containers having nonconical shapes. The use of precisely tapered vacuum-formed fused quartz growth ampoules can obviously be extended to more complex geometries depending on specific application requirements.

5. Summary of Results

Precisely-tapered square or round cross section fused quartz growth ampoules, dense pyrolytic carbon coatings, and c-axis seeding have permitted the growth of high quality crystals of $AgGaSe_2$ in spite of anomolous thermal expansion along its optic axis during cooling. Cutting yields are significantly improved in the manufacture of 1 cm^2 nonlinear optical crystals in multi-centimeter lengths by growing the boules with square rather than circular cross-section. True costs must include the use of somewhat more expensive square cross-section growth ampoules which can be reused only if care is taken to prevent chemical reaction with the melts during growth. The vacuum-forming technology to produce precisely tapered fused quartz growth ampoules is readily adaptable to small glass lathes with moderate size multiple burner cross-fire torches.

TABLE II

Difference in Cutting Yields between Circular and Square Cross-Section Boules in the Manufacture of 1 cm Thick Slabs.

Boule Dimensions	1 cm Thick Slabs Out	Total (Cross-Section)	Yield (Cross-Section)	Kerf Loss (Cross-Section)	Recoverable Fraction
30 mm dia	2	707 mm^2	420 mm^2	105 mm^2	26%
21 mm^2	2	441 mm^2	420 mm^2	21 mm^2	-0-
45 mm dia	3	1590 mm^2	960 mm^2	160 mm^2	30%
32 mm^2	3	1024 mm^2	960 mm^2	64 mm^2	-0-

D. CHEMICAL INTERDIFFUSION STUDIES IN THE $AgSe$-Ga_2Se_3 SYSTEM

In sections A and B, we reviewed the heat-treatment procedure that is used to eliminate optical scattering precipitates from as-grown $AgGaSe_2$ crystals. The purpose of the research described in this section is to gain a better understanding of the chemical reactions, the reaction pathways, and the reaction kinetics that occur during the heat-treatment procedure.

1. Background

The identity of the precipitates in as-grown $AgGaSe_2$, has been established as $AgGaSe_2$ saturated with Ga_2Se_3, of approximate composition $AgGa_7Se_{11}$. The "phase" $AgGa_7Se_{11}$ is not rigorously a compound, but merely represents the extent of terminal solid solubility of Ga_2Se_3 saturated with $AgGaSe_2$, as established by Mikkelsen.[14] Figure 25 shows the condensed phase equilibria in the pseudobinary Ag_2Se-Ga_2Se_3 system. While this approximation is not strictly correct because two of the three constituents, gallium and selenium, are known to transport through the vapor phase, it is useful in interpreting the heat-treatment process. Referring back to Fig. 12, the current heat-treatment procedure consists of encapsulating as-grown crystals of $AgGaSe_2$ (which contain $AgGa_7Se_{11}$ precipitates) in a vacuum-sealed fused quartz ampoule along with a small amount of Ag_2Se. Soaking at 800° C for 14-21 days allows chemical interdiffusion to occur. The 800° C join, X-Y in Fig. 25, represents the diffusion couple between Ag_2Se(X) and an as-grown $AgGaSe_2$ crystal (Y) which is formed during the procedure. The phase field identified as β is single phase $AgGaSe_2$ with excess Ga_2Se_3 in solution. If the as-grown crystal (Y) is cooled to room temperature along the isoconcentration line Y-Z, the result is $AgGaSe_2$ as the major phase and δ ($AgGa_7Se_{11}$) as the precipitate phase. By reheating as-grown crystals (Z) back into the single phase region at Y (800° C), the precipitates dissolve back into the lattice. The overall composition of the now single phase, defect-free crystals can be modified by chemical interdiffusion to a composition from which precipitation does not occur as they are cooled to room temperatures. The objective then, during heat-treatment is to adjust the composition of the crystal to the Ag_2Se_3-rich boundary at Y' which we have determined empirically is very close to true stoichiometry. The crystals then cool along Y'-Z' and end up at Z', free of precipitates.

A complicating factor is that chemical exchange between the two members of the diffusion couple, illustrated in Fig. 12, occurs both through the vapor phase and through

the solid phase. Indeed, complete elimination of precipitates in the related compound $AgGaS_2$ can be accomplished with vapor phase communication alone. This does not seem to be possible with $AgGaSe_2$. Direct physical contact during at least some of the heat-treatment cycle is found to be necessary for optimum results even though chemical exchange of both gallium and selenium does occur through the vapor phase. Not understanding the reason(s) for this, we have sought to elucidate the chemical reactions, the reaction pathways, and the reaction kinetics in a series of diffusion experiments.

2. Experimental Procedures

Several sets of diffusion experiments have been carried out under the conditions outlined in Table III.

TABLE III

Temp. Range	Heat-Treatment Medium	
	Mechanical Contact plus Vapor Phase Contact	Vapor Phase Contact Only
800° C	---	None
800° C	Ag_2Se	Ag_2Se
670° C	Ag_2Se	Ag_2Se
300-600° C	Ag_9GaSe_6	---

Samples of as-grown $AgGaSe_2$ along with predetermined amounts of an annealing medium; either nothing, Ag_2Se, or Ag_9GaSe_6; were sealed in evacuated fused quartz ampoules under conditions of both intimate mechanical contact and no mechanical contact. Samples of similar size were selected whenever we were attempting to differentiate between mass transported through the vapor phase and mass transported through the solid phase. Reaction times varied from 2.5 - 14 days. Afterward, the heat-treatment ampoules were slowly cooled to room temperature.

Mass fractions transported through the vapor phase in the non-contact cases were determined by careful weighing techniques. Phases present were identified by x-ray diffraction analysis using powder XRD, and 4-circle step-scan XRD in the cases where minor second phases were expected to be present after heat-treatment only as thin layers on the surfaces of the crystals.

3. Results

As mentioned in section B, in all heat-treatment processing carried out at 800° C, the annealing media was found to have formed a liquid phase by chemical reaction. Only where mechanical contact between the $AgGaSe_2$ crystals and the annealing medium was prevented was it possible to determine accurately the mass transport that took place. In the experiments where mechanical contact occurred, the liquid phase in contact with the $AgGaSe_2$ crystal created a metallurgical junction. Extensive cracking of the $AgGaSe_2$ crystals always occurred in this region during cooling due to differential thermal expansion. For this reason, it was difficult to quantify compositional variations on either side of this junction. In the series of experiments carried out at temperatures below the lowest eutectic in the binary system (728° C), a liquid phase did not form and it was possible to study the metallurgical junctions. This particular research study is still in progress.

4. Discussion

Generally, we are attempting to analyze the two cases illustrated in Fig. 26 and 27, where no contact occurs and where contact occurs, respectively. The problem is quite complicated since diffusion occurs through two solid phases, a liquid phase and the vapor phase. Furthermore, we do not know the exact molar fraction, m, of the $AgGa_7Se_{11}$ precipitate phase since it varies from crystal to crystal depending on where in the as-grown boule each was harvested. Some simplifications are therefore necessary.

a. Thermodynamic Equilibrium

In the cases studied, where 800°C heat-treatment has exceeded more than a few days in length, XRD phase identification has revealed only the phases shown on the binary phase equilibria, Fig. 25. One may conclude that the system remains binary and that gallium and selenium transport through the vapor phase in 2:3 (Ga_2Se_3) stoichiometric proportion. In all cases, the system appears to equilibrate on the binary join, X-Y. To achieve the desired composition of the β phase (at Y') the system must be forced to

equilibrate in the (β + L) phase field along the Z-Y' join. This places a maximum limit on the amount of Ag_2Se or Ag_9GaSe_6 annealing media used in heat-treatment processing of optical crystals. In a practical sense, one would choose to use the minimum amount of annealing media necessary to equilibrate the system along the Z-Y' join, on the order of a mole percent or less. In other words, one would choose to end up as close to Y' as possible, but definitely in the two phase side of the boundary.

To elucidate the chemical reactions taking place during the heat-treatment process, larger quantities of annealing media were utilized in many of our experiments.

b. Kinetic Analysis

(1.) Assumptions of the Analysis

a) The precipitates which occur during the crystal growth of $AgGaSe_2$ have the composition of $AgGa_7S_{11}$.

b) The dissolution of the precipitates is as follows:

$$AgGa_7Se_{11} \xrightarrow{800^\circ C} AgGaSe_2 + 6\,Ga^{3+} + 9\,Se^{2-} \qquad (1)$$

c) The Ga and Se atoms, as a result of the dissolution of the precipitates, diffuse through the $AgGaSe_2$ crystal lattice by a substitutional mechanism. We deduce this from the diffusivity data in GaAs which has similar chemical bonding.[25]

d) Ag_2Se as the annealing medium is in equilibrium with Ag and Se as follows:

$$Ag_2Se \underset{\rightarrow}{\leftarrow} 2\,Ag^{+} + Se^{2-} \qquad (2)$$

e) Silver is known to diffuse rapidly at only moderate temperatures in ionic compounds such as Ag_2S, which is very similar to Ag_2Se.[26] Diffusion is assumed to occur by an interstitial mechanism. Therefore, when direct mechanical contact occurs, the Ag atoms should be able to diffuse from the Ag_2Se into the $AgGaSe_2$ sample in this manner. When no physical contact occurs, we assume that Ag does not transport through the vapor phase.

f) Vapor phase transport is assumed to be faster than substitutional diffusion of Ga and Se at the heat-treatment temperatures used. Hence, we ignore

substitutional diffusion of Ga and Se from the $AgGaSe_2$ sample into the Ag_2Se annealing medium even when mechanical contact is present. This is probably a fair assumption since the relative area of $AgGaSe_2$ in contact with the vapor phase far exceeds that in mechanical contact with the annealing medium. The vapor pressure of atomic Ga at the temperatures used (670° C and 800° C) is not consistent with mass transport through the vapor phase. Selenium has a relatively high vapor pressure, however, and it is thought that Se atoms complex the Ga atoms during the vapor transport process.

(2.) Proposed Reactions

a) When there is no contact between the sample and the annealing medium, there are four possible rate limiting steps, (1) dissolution of $AgGa_7Se_{11}$, (2) diffusion of the excess Ga and Se atoms to the surface of the sample, (3) vapor transport of the Ga and Se atoms, and (4) chemical reaction on the surface of the annealing medium. These steps are in series and so the overall reaction rate depends on the slowest step. Fig. 26 illustrates this case.

In the sample, the following dissociation reaction occurs:

$$m\ AgGa_7Se_{11} \xrightarrow{800^\circ C} m\ AgGaSe_2 + 6\ m\ Ga^{3+} + 9\ m\ Se^{2-} \qquad (3)$$

As a result, the excess Ga and Se atoms are free to diffuse throughout the sample to the surface where they vaporize and recondense on the annealing medium because of the difference in chemical potential. The magnitude of the mass transmittance will depend on the diffusion of Ga and Se through the $AgGaSe_2$ sample and the flux via transport through the vapor phase.

In the annealing medium, thermodynamic equilibrium will result in some ionic silver being available to react with excess Ga and Se atoms reaching its surface via vapor phase transport.

$$j\ Ag_2Se \xrightarrow{800^\circ C} 2\ Ag^{+} + Se^{2-} \qquad (4)$$

b) When there is contact between the sample and the annealing medium, there are two reaction paths we need to consider:

(i) *path 1* - dissolution of $AgGa_7Se_{11}$ to make Ga and Se atoms → diffusion of excess Ga and Se atoms through the sample to its surface → vapor transport → chemical reaction of the excess Ga and Se atoms, with the annealing medium.

(ii) *path 2* - decomposition of Ag_2Se → diffusion of Ag^+ (and Se^{2-}) from the annealing medium into the $AgGaSe_2$ sample → chemical reaction between the Ag, Ga and Se atoms.

Each path has its own reaction rate-determining step and which path dominates depends on partitioning of the four parameters (k, t, n and m) defined below. Fig. 27 illustrates this case, where

m: number of moles of $AgGa_7Se_{11}$ initially

n: number of moles of Ag_2Se reacted with vapor transported Ga and Se

k: number of moles of Ag_2Se diffused into the $AgGaSe_2$ sample

t: number of moles of initial $AgGa\ Se_2$

W_{osi}: initial weight of the sample for contactless case

W_{osf}: final weight of the sample for contactless case

W_{csi}: initial weight of the sample for contact case

W_{csf}: final weight of the sample for contact case

W_{cmi}: initial weight of the medium for contact case

W_{cmf}: final weight of the medium for contact case

W_{omi}: initial weight of the medium for the contactless case

W_{omf}: final weight of the medium for the contactless case

From mass balance, the following equations hold:

$$W_{osi} - W_{osf} = 3\,m\,D \quad (5)$$

$$W_{csi} = t\,A + m\,B \quad (6)$$

$$W_{csf} = (t + m)\,A + k\,C \quad (7)$$

$$W_{cmi} = (k + n)\,C \quad (8)$$

$$W_{cmf} = n\,C + 3\,m\,D \quad (9)$$

where A, B, C and D represent the molecular weights of $AgGaSe_2$, $AgGa_7Se_{11}$, Ag_2Se and Ga_2Se_3, respectively. Solving the above equations,

$$m = \frac{W_{osi} - W_{osf}}{3\,D} \quad (10)$$

$$t = \frac{W_{csi} - m\,B}{A} \quad (11)$$

$$k = \frac{W_{osf} - (t + m)\,A}{C} \tag{12}$$

$$n = \frac{W_{crni}}{C} - k \tag{13}$$

Initially, dissolution of $AgGa_7Se_{11}$ precipitates occurs.

$$(m+q)\ AgGa_7Se_{11} \rightarrow (m+q)\ AgGaSe_2 + 6\,(m+q)\ Ga^{3+} + 9\,(m+q)\ Se^{2-} \tag{14}$$

Also, Ag_2Se will decompose to Ag^+ and Se^{2-} as follows:

$$jAg_2Se \rightarrow 2k\ Ag^+ + k\ Se^{2-} + 2n\ Ag^+ + n\ Se^{2-} \tag{15}$$

The decomposed elements are partitioned into *path 2*. Of the two reactions that can occur in the sample,

$$(m+t)\ AgGaSe_2 + 2k\ Ag + k\ Se \rightarrow \frac{4\,(m+t) - k}{4}\ AgGaSe_2 + \frac{k}{4}\ Ag_9GaSe_6 \tag{16}$$

$$\text{where } 0 \le k \le 4\,(m+t)$$

Likewise, the reaction occurring in the annealing medium is

$$6m\ Ga + 2\,n\ Ag + (9\,m + n)\ Se \rightarrow \frac{7\,n - 3\,m}{3}\ AgGaSe_2 + \frac{3\,m - n}{3}\ AgGa_7Se_{11}, \tag{17}$$

$$\text{where } \frac{3\,m}{7} \le n \le 3\,m$$

The constraints are made in order to equilibrate the system along the W - Y' join in Fig. 25.

c.) Experimental Example - no mechanical contact

The $AgGaSe_2$ sample used for annealing was grown at the normal growth rate (6 mm/day) using the Bridgman technique. The annealing conditions are shown in Table IV.

TABLE IV

Annealing condition for contactless case

	Before Heat-Treatment	After Heat-Treatment
Weight of the sample	5.3427 g	5.3097 g
Weight of Ag_2Se	0.0710 g	0.1029 g
Annealing Temperature	800° C	800° C
Annealing Time	2.5 days	2.5 days
Furnace Type	horizontal type	horizontal type
Annealing Environment	vacuum (1.5×10^{-3} torr)	vacuum(1.5×10^{-3} torr)

The sample lost 0.033 g during the experiment, while the annealing medium gained 0.0319 g during the experiment. The discrepancy between these two values was thought to be due to material deposited on the quartz tube after annealing. According to our model, the dissolution of $AgGa_7Se_{11}$ precipitates dissolve in the matrix phase at these high annealing temperatures and, as a result, excess Ga and Se exist in the matrix. Since there is no physical contact, we do not have to take into account the solid diffusivities of either species. We can roughly estimate the flux of each species as follows:

$$J\ (Ga_2Se_3) = 8.769 \times 10^{-5}\ \text{moles}/[(\pi \times 2.5\ 2/4)\ \text{cm}^2\ (2.5 \times 86400\ \text{sec})]$$
$$J\ (Ga_2Se_3) = 8.27 \times 10^{-9}\ \text{moles/cm}^2\ \text{sec.} \qquad (18)$$

By assuming stoichiometry,

$$J\ (Ga) = 1.65 \times 10^{-8}\ \text{moles/cm}^2\ \text{sec} \qquad (19)$$

$$J\ (Se) = 2.48 \times 10^{-8}\ \text{moles/cm}^2\ \text{sec} \qquad (20)$$

X-ray step scan analysis showed that there were no additional phases on the surface of the $AgGaSe_2$ sample. This verified the direction of mass transport. In the sample, the only phase detected was $AgGaSe_2$. (There were not enough $AgGa_7Se_{11}$ precipitates in the sample to be detected by X-ray analysis.)

The chemical identification of the x-ray peaks in the annealing medium is shown in Table V.

TABLE V

X-ray diffraction data of the annealing medium for contactless case

d_{obs}	I/I_0	hkl($AgGaSe_2$)	hkl (Ag_9GaSe_6)
3.335	100	112	---
3.209	25	---	222
2.599	11	211	---
2.555	13	---	331
2.143	16	---	333 or 511
2.119	38	220	---
2.014	58	222	---
1.968	15	---	440
1.790	28	312	---
1.668	13	321	---

Since there were only two kinds of intermetallic compounds present, $AgGaSe_2$ and Ag_9GaSe_6.

$$6m\ Ga + (9\ m+j)\ Se + 2j\ Ag \rightarrow \frac{27\ m - j}{4}\ AgGaSe_2 + \frac{j - 3\ m}{4}\ Ag_9GaSe_6. \qquad (21)$$

From the weight change of the sample we can calculate m and J,

$$m = 2.923 \times 10^{-5} \text{ mole} \qquad (22)$$

$$J = 2.41 \times 10^{-4} \text{ mole} \qquad (23)$$

Since the amount of the original $AgGaSe_2$ sample was 1.58×10^{-2} mole and the calculated amount of dissolved precipitates was 2.923×10^{-5} mole, we conclude that 0.185 mole% of the original $AgGaSe_2$ crystal consisted of the precipitate phase, $AgGa_7Se_{11}$. In this analysis we have assumed thermodynamic equilibrium and that all of the precipitates were gone after annealing. Converting this to system mole fractions, we calculate that the overall chemical composition of the crystal, before annealing, was 49.35% Ag_2Se -

50.65% Ga_2Se_3, slightly more than 1/2 mole percent rich in Ga_2Se_3. This is quite close to the empirical estimate made by ourselves and others.[24]

In the $AgGaSe_2$ crystal, dissolved excess Ga and Se should diffuse to the surface by a vacancy mechanism. This step depends on the annealing temperature and annealing time, and the overall diffusion will be governed by the species whose diffusivity is slower. If we can determine the diffusivities for Ga and Se atoms, then we can estimate the total concentration of the precipitates remaining in the sample as a function of time, in other words, understand the kinetics of the heat-treatment process. This information should be obtainable from a quantitative analysis of chemical interdiffusion when physical contact occurs, and when temperatures are low enough that vapor phase transport can be neglected.

d.) Experimental Example - mechanical contact

With mechanical contact occurring, we must take into account the additional diffusion component occurring through the solid phase. Tracer diffusivity measurements would provide useful data which we do not now have. These are difficult to carry out in multi-component systems. When intermediate phases or intermetallic compounds are formed during diffusion, analysis is complicated.[28] The role of any intermediate phase is to modify the diffusion process. We have chosen to substitute Ag_9GaSe_6 as the annealing medium since Ag_9GaSe_6 forms anyway, early in the heat-treatment procedure, and we have set out to analyze interdiffusion in the somewhat simpler Ag_9GaSe_6 - $AgGa_7Se_{11}$ system.

1) For mathematical convenience, diffusion in a two-component system is usually treated using the simple Fick's laws and a single interdiffusion coefficient D. Since D includes many of the complexities of the diffusion process, it often varies with composition. In case of the three-component system, the concentration gradient of any component can affect the diffusion flux of component 1, leading to the equation

$$J_1 = \tilde{D}_{11}\frac{\delta C_1}{\delta x} - \tilde{D}_{12}\frac{\delta C_2}{\delta x} - \tilde{D}_{13}\frac{\delta C_3}{\delta x} \qquad (28)$$

Similar equations can be written for J_2 and J_3, the fluxes of the other two components. Since $C_1 + C_2 + C_3 = 1$, equation (28) can be reduced as follows:

$$J_1 = \tilde{D}^3_{11}\frac{\delta C_1}{\delta x} - \tilde{D}^3_{12}\frac{\delta C_2}{\delta x} \qquad (29)$$

where $\tilde{D}^k_{ij} = \tilde{D}_{ij} - \tilde{D}_{ik}$.. In view of the definition of the Matano interface, $J_1 + J_2 + J_3 = 0$, and therefore the flux of component 3 is also a dependent quantity. The flux of component 2 is given by

$$J_2 = \tilde{D}^3_{21}\frac{\delta C_1}{\delta x} - \tilde{D}^3_{22}\frac{\delta C_2}{\delta x} \qquad (30)$$

and therefore, a total of four diffusion coefficients is adequate to describe the diffusion behavior of a three-component system. In this method, the diffusion path follows a curved line and the interpretation is not easy. But,if we treat the three-component system as a pseudobinary system, we can get the interdiffusion coefficient using the improved Matano-Boltzmann analysis, which was developed by F. J. A. den Broeder.[29]

This method makes it possible to calculate the interdiffusion coefficients without the necessity identifying the original interface, which makes the analysis easier and more accurate, although it still involves calculation of the slope and the area of the concentration profile.

2) Experimental Setup

A conventional diffusion couple will ultimately be prepared between Ag_9GaSe_6 and a dense polycrystalline sample of $AgGa_7Se_{11}$. Ceramic markers will identify the original boundary. In a preliminary experiment, a conventional diffusion couple has been made by clamping polycrystalline Ag_9GaSe_6 together with a precipitate-free $AgGaSe_2$ crystal with a quartz spring. The synthesis of the polycrystalline Ag_9GaSe_6 was carried out by direct fusion.

Since both samples have the same elements, if they are in contact, the equilibrium concentration of each element will be reached when the chemical potentials of each element between the two samples are the same. After the quartz ampoule which contains two samples was evacuated and sealed, annealing was carried out at selected temperatures, from 300° C to 600° C. The diffusion couples were then removed from the ampoules, mounted

in epoxy resin, and prepared for electron microprobe analysis (EPMA). (These studies are now underway.)

Early diffusion experiments well below the eutectic temperature resulted in extensive reaction on the surface of the $AgGaSe_2$ and the apparent formation of the Ag_9GaSe_6 phase. Of the two possible mechanisms, surface diffusion and vapor phase transport of Ga_2Se_3, significant vapor transport seems less likely at such low temperatures. We are currently in the process of additional phase identification studies by XRD, and additional EPMA studies to elucidate this effect. Following this, we plan to complete the proposed Ag_9GaSe_6 - $AgGa_7Se_{11}$ diffusion studies using a ceramic boundary marker as an aid in sorting out the relative diffusion rates through the intermediate $AgGaSe_2$ phase which should form and grow by solid diffusion where the two end members meet.

E. INFLUENCES OF COUPLED VIBRATIONAL STIRRING DURING BRIDGMAN GROWTH OF $AgGaSe_2$

1. Background

During the growth of $AgGaSe_2$ crystals by the vertical Bridgman method, direct stirring is impossible because the material is contained in a sealed ampoule. Yet it is desirable to do so, if possible, because the off-stoichiometric congruency in this system means that in growth from stoichiometric melts, there is a compositional diffusion boundary layer ahead of the growth interface. Excess Ag_2Se-rich material must diffuse back into the melt, or be incorporated as a second phase or in solid solution. To reduce the occurrence of discrete Ag_2Se-rich inclusions, forced convection (stirring) is desirable. As a part of this program, a series of four crystal growth experiments was carried out, two with forced melt convection (stirring) and two without. Growth rates were normal and 4 times normal in both cases.

2. Experimental Procedures

Melt stirring was accomplished by coupled vibrational stirring (CVS), which has been shown to be a very effective mixing method.[29] CVS provides a very rapid spiral fluid flow down the walls of the ampoule and a corresponding flow up the center of the melt. Stirring is accomplished by moving the entire sealed fused quartz growth ampoule in a circular motion in the horizontal plane. Rotational motion about the axis of the growth ampoule is prevented by a spring restraint. A planar air bearing apparatus with eccentric mechanical drive is used to generate the desired motion. Components of the assembly are shown in Fig. 28. The distance between the center of the drive pin and the center of the motor shaft was 1/8 inch, which gave a fixed transverse vibrational amplitude. The vibrational frequency was varied by changing the motor speed. Modelling work was done at room temperature with a water-glycerol solution of viscosity 2.5 c.p., the estimated viscosity of molten $AgGaSe_2$, using black ink injected at the bottom of the test container. A laser and a photodector were used to determine the total mixing time. Mixture heights equivalent to the heights of the melt in a 25 mm diameter growth ampoule (approximately 10 cm) were used to simulate the crystal growth of $AgGaSe_2$. Later, an uncoated sealed growth ampoule charged with $AgGaSe_2$ and a one-zone transparent furnace were used to observe at temperature, the height of the surface wave induced in molten $AgGaSe_2$ by the precessional motion. Conditions below the resonance frequency of the melt crucible system, where the surface wave amplitude is a maximum,

were chosen for the actual crystal growth experiments to limit transverse inertial forces on the growth ampoules.

3. Results

The results of these experiments were dramatic. The two crystals grown at 4 x normal growth rate showed a striking effect: the one grown without CVS as a control boule contained many cellular boundaries caused by a totally unstable growth interface; the one grown with CVS slowed only a few cell boundaries indicating a significantly more stable growth interface, Fig. 29. We feel this demonstrates that forced melt stirring by CVS adds to growth interface stability in $AgGaSe_2$. Little difference was observed between the crystals grown at the normal growth rate, suggesting nothing deleterious is caused by CVS.

4. Discussion

The loss of one of the four crystals due to inappropriate handling during chem-mechanical polishing has prevented us from completing a careful comparison of the residual optical scatter/absorption in these four crystals. With subsequent support from the Army Research Office, we are in the process of extending this research by regrowing the lost crystal and carrying out the same comparisons on crystals grown at 2 x and 3 x the normal growth rate. Results of these studies when they are completed will be reported in the scientific literature with appropriate acknowledgement of support.

III. CONCLUSIONS AND RECOMMENDATIONS FOR FUTURE RESEARCH

The complete story of $AgGaSe_2$ cannot be written yet but this program, even though it was severely reduced in support level, has added significantly to our scientific and engineering knowledge of this material system. The program has been very successful in that significant publishable advances in three of its five component areas have been achieved. 1) A far superior understanding of residual optical scattering centers and processes to eliminate them is now in hand, 2) Boules 37 mm in diameter yielding optical crystals up to 40 mm in length are routine, and 3) Square cross-section crystals have been shown to be feasible using vacuum-formed quartz ampoule technology, and their much higher fabrication yields should be an attractive feature for commercial processing. Additional research is yet to be completed in the two student dissertation research areas: elucidation of the chemical interdiffusion process(es) occurring during heat-treatment, and a comprehensive assessment of the effects of indirect melt stirring by the CVS method.

Further experience in the operation of optical parametric oscillators and resonant harmonic generators, and detailed power balance measurements, both beyond the scope of this program, are needed to verify that we now understand the main causes of residual optical absorption on this material. Continuing cooperation between Stanford and research staff from the Naval Research Laboratories is directed toward resolving some of these issues. There is still room for additional phase equilibrium and heat-treatment studies coupled more tightly with device evaluation, and such support is urged. It is particularly important to learn as much as possible about semiconducting chalcogenide systems such as Ag-Ga-Se as they are among the few systems which possess useful linear and nonlinear optical properties in the infrared.

$ZnGeP_2$, a related compound is known to possess higher nonlinear coefficients than the materials described above. Although its useful transparency range is not as great, continuing support for the growth and characterization of this important material should be pursued.

IV. REFERENCES

1. R. L. Byer, "Nonlinear optical phenomena and materials," Annual Review of Materials Science, Annual Reviews, Inc., Palo Alto, CA, vol.4, 147 (1974).

2. G. D. Boyd, H. M. Kasper, J. H. McFee, and F. G. Stortz, "Linear and nonlinear optical properties of some ternary selenites," IEEE J. Quantum Electron. QE-8(12), 900-908 (1972).

3. H. Kildal and J. C. Mikkelsen, "The nonlinear optical coefficient, phasematching, and optical damage in the chalcopyrite $AgGaSe_2$," Opt. Commun , 315-318 (1973).

4. G. C. Bhar and R. C. Smith, "Optical properties of II-IV-V2 and I-III-VI2 crystals with particular reference to transmission limits," Phys. Status Solidi. A: 13(1), 157-168 (1972).

5. R. L. Byer, M. M. Choy, R. L. Herbst, D. S. Chemla, and R. S. Feigelson, "Second harmonic generation and infrared mixing in $AgGaSe_2$," Appl. Phys. Lett. 24(2), 65-68 (1974).

6. G. W Iseler, "Thermal expansion and seeded Bridgman growth of $AgGaSe_2$," J. Cryst. Growth 41(1), 146-150 (1977).

7. B. Tell and H. M. Kasper, "Optical and electrical properties of $AgGaS_2$ and $AgGaSe_2$," Phys. Rev. B: 4(12), 4455-4459 (1971).

8. H. M. Kasper, "Crystal growth and properties of some I-III-IV2 compounds," Nat. Bur.Std, (U.S) Spec. Publ. 364, 671-679 (1972).

9. R. K. Route, R. S. Feigelson, and R. J. Raymakers, "Growth of $AgGaSe_2$ for infrared applications," J. Cryst. Growth 24/25, 390-395 (1974).

10. R. K. Route, R. J. Raymakers, and R. S. Feigelson, "Preparation of large untwinned single crystals of $AgGaS_2$ and $AgGaSe_2$," J. Cryst. Growth 29(1), 125-126 (1975).

11. H. Matthes, R. Viehmann, and N. Marschall, "Improved optical quality of $AgGaS_2$," Appl. Phys. Lett. 26(5), 237-239 (1975).

12. R. K. Route, R. S. Feigelson, and R. J. Raymakers, "Elimination of optical scattering defects in $AgGaSe_2$," J. Cryst. Growth 33(2), 239-245 (1976).

13. L. S. Palatnik and E. K. Belova,"Izv. Akad. Nauk, SSSR Neorg. Mater. 3, 2194 (1967).

14. J. C. Mikkelsen, Jr., "Ag_2Se-Ga_2Se_3 pseudobinary phase diagram," Mater. Res. Bull. 12(5), 497-502 (1977).

15. R. S. Feigelson, R. Koch, R. K. Route, and C.-E. Huang, "Defects in the ternary chalco-pyrites $AgGaS_2$ and $AgGaSe_2$," in collected abstracts, IOCG VII Int. Conf. on Crystal Growth, Stuttgart, Germany (1983).

16. N. B. Singh, R. H. Hopkins and J. D. Feichtner "Effect of annealing on the optical quality of $AgGaS_2$ and $AgGaSe_2$ single crystals," J. Mat. Sci. 21, 837 (1986).

17. N. B. Singh, R. H. Hopkins, R. Mazelsky, and H. H. Dorman, "Annealing experiments on silver gallium selenide crystals," Materials Lett. 4, 357 (1986).

18. G. Brandt and V. Krämer, "Phase investigations in the silver-gallium-sulfur system, Mater. Res. Bull. 11(11), 1381-1388 (1976).

19. R. C. Eckardt, Y. X. Fan, R. L. Byer, C. L. Marquardt, M. E. Storm and L. Esterowitz, "Broadly tunable infrared parametric oscillator using $AgGaSe_2$," Appl. Phys. Lett. 49(11), 608-613 (1986).

20. R. C. Eckardt, Y. X. Fan, R. L. Byer, R. K. Route, R. S. Feigelson, and J. van der Laan, "Efficient second harmonic generation of 10-μm radiation in $AgGaSe_2$," Appl. Phys. Lett.47(8), 786-788 (1985).

21. R. C. Eckardt, R. L. Byer, L. A. Newman and J. Kennedy, "High-average-intensity nonlinear infrared frequency conversion in AgGaSe2," paper WM33, Proc. Conference on Lasers and Electro-Optics, Anaheim, CA (April 1988).

22. R. S. Feigelson and R. K. Route, "Recent developments in the growth of chalcopyrite crystals for nonlinear infrared applications," Opt. Eng. 26 (2), 837 (1986).

23. R. C. Echkardt, private communication.

24. L. Shiozawa and J. Heitanen, Cleveland Crystals, Inc., private communication.

25. R. S. Feigelson and R. K. Route, "Improvements in the optical quality of silver selenogallate ($AgGaSe_2$) crystals," to be published in J. Crystal Growth (1989).

26. E. E. Hellstrom and R. A. Huggins, "Silver Ionic and Electronic Conductivity in Ag_9GaS_6, Ag_9AlS_6, $AgGaS_2$, $AgAlS_2$ and $AgAl_5S_8$," J. Solid State Chem. 35, 207 (1980).

27. C. Wagner, J. Chem. Phys. vol. 21, 1819-1827 (1953).

28. Stanislaw Mrowec, Defects and Diffusion in Solids, pp. 283-286 (Elsevier 1979).

29. F. J. A. den Broeder, J. Scripta Metallurgica 3, 321-325 (1969).

30. W.-S. Liu, M. F. Wolf, D. Elwell and R. S. Feigelson, "Low frequency vibrational stirring: A new method for rapidly mixing solutions and melts during growth,", J. Crystal Growth 82, 589-597 (1987).

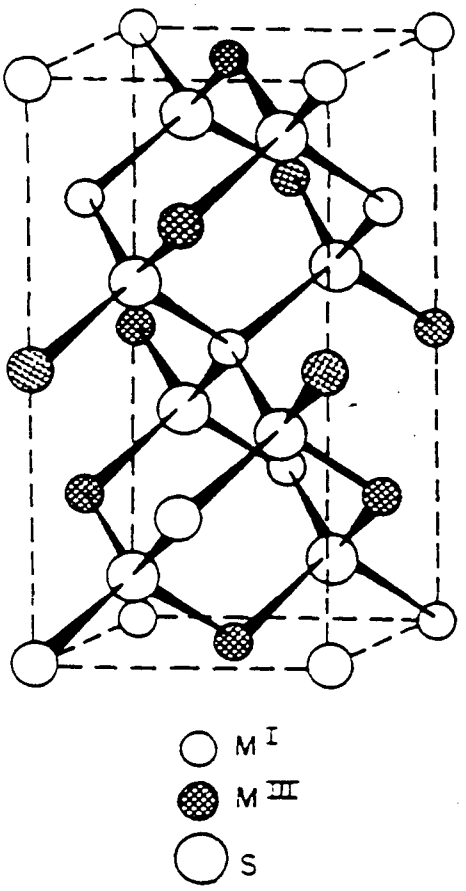

Fig. 1. Unit cell of the chalcopyrite structure.

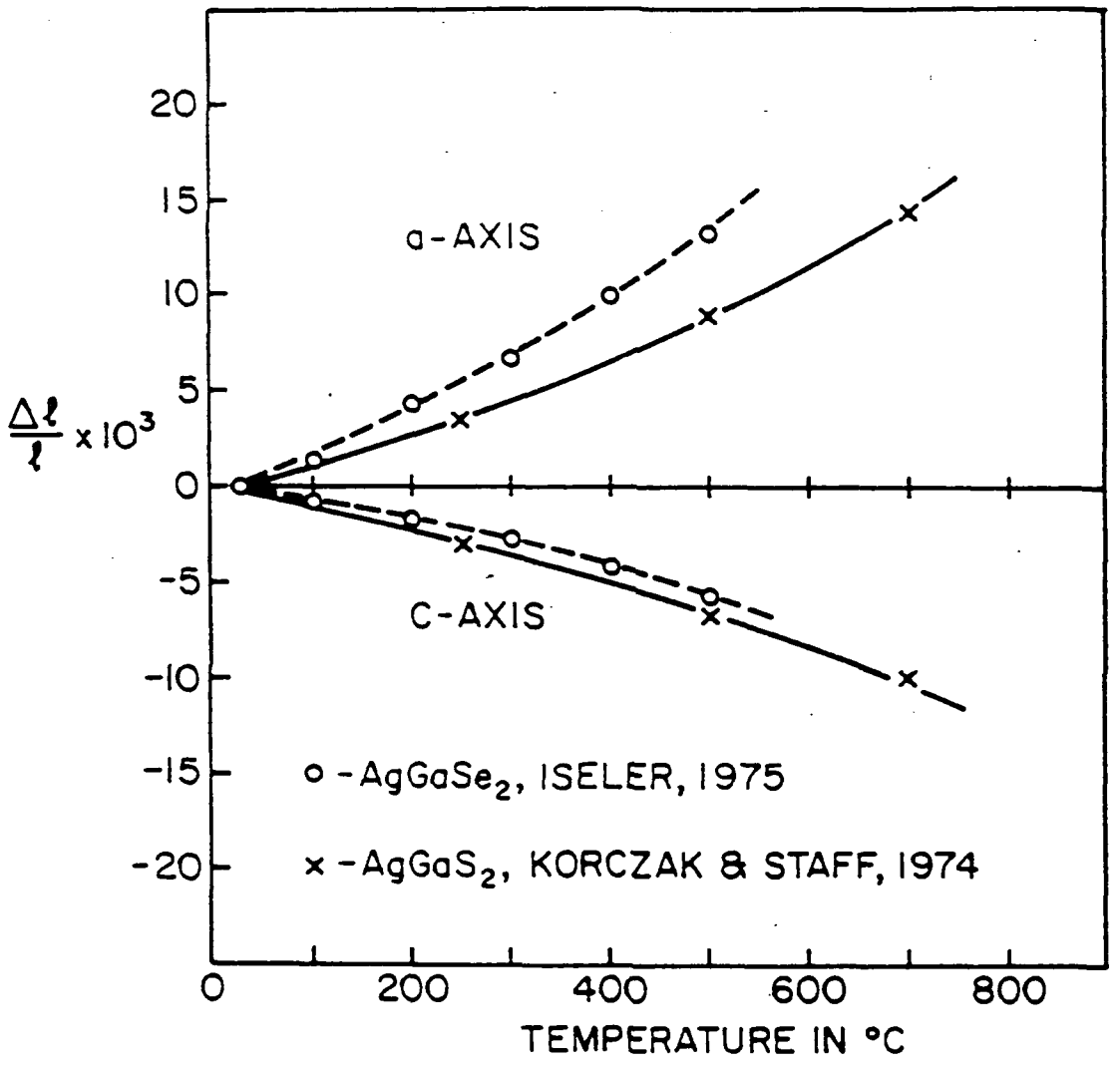

Fig. 2. Thermal expansion properties showing anomalous behavior along the c-axis.

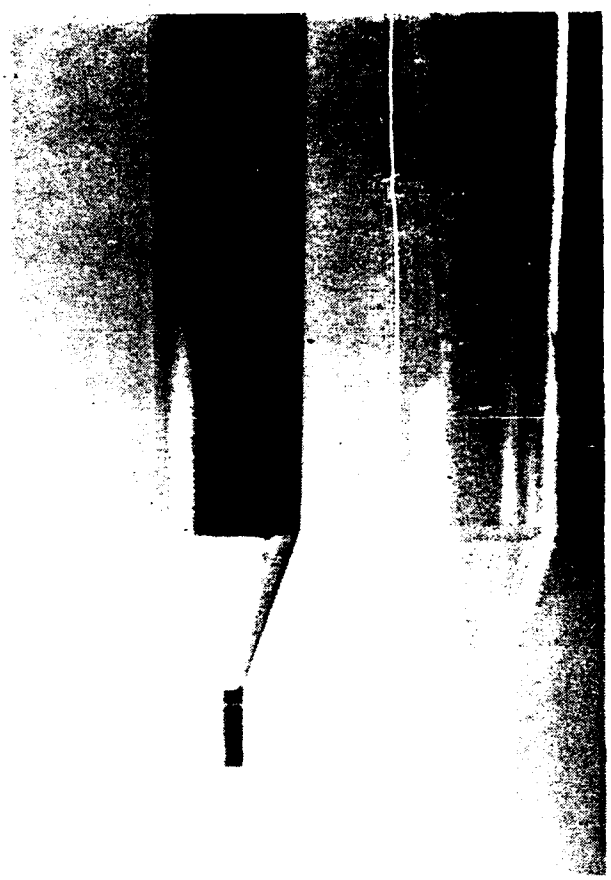

Fig. 3. Precision tapered graphite mandrel and vacuum-formed fused-quartz growth ampoule.

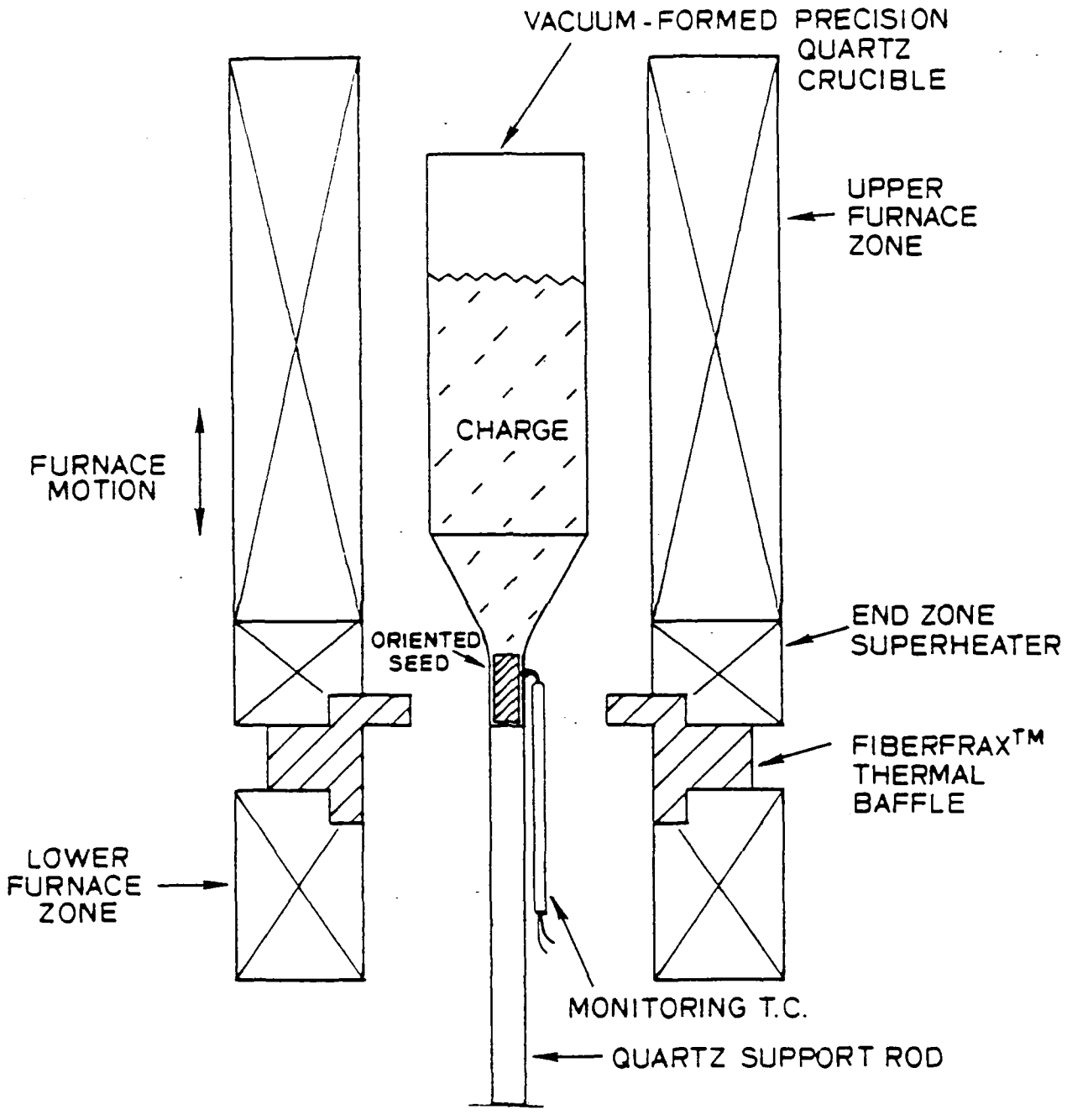

Fig. 4. Bridgman furnace configuration showing thermocouple monitor by which meltback and seed attachment are controlled.

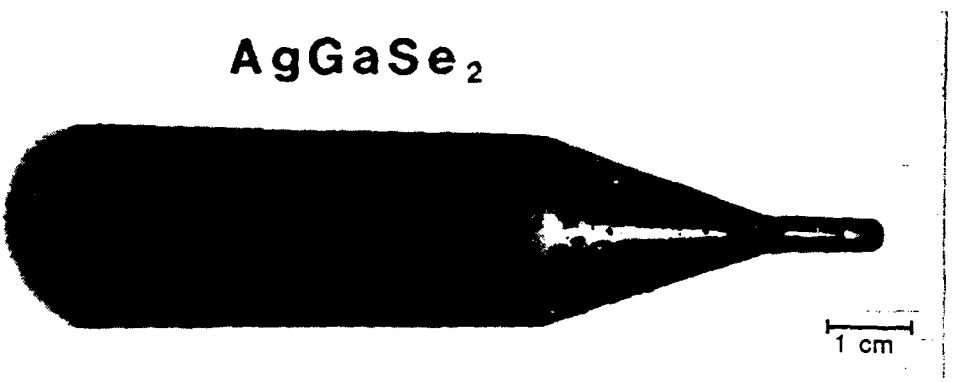

Fig. 5. 28 mm twin - and crack-free boule in $AgGaSe_2$.

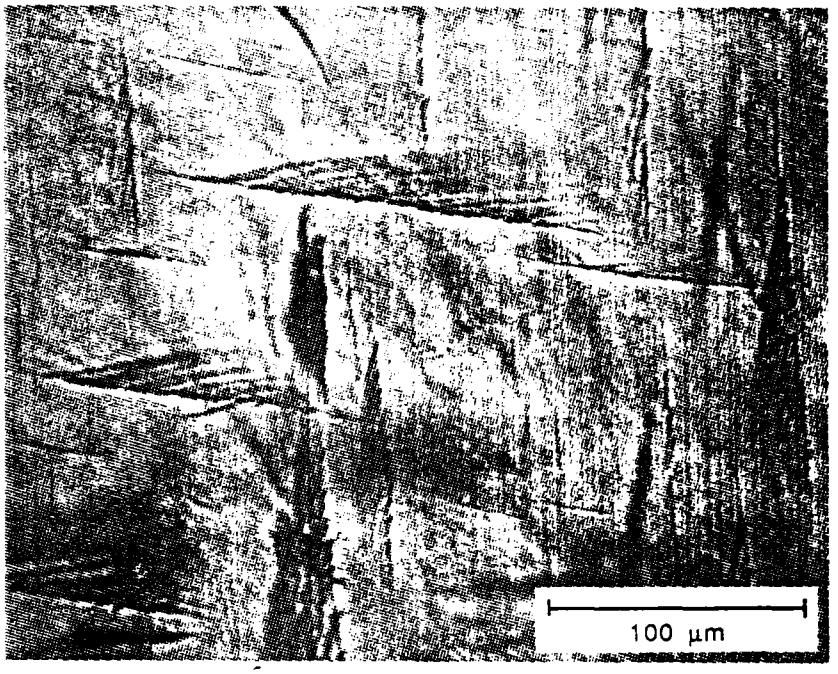

(a)

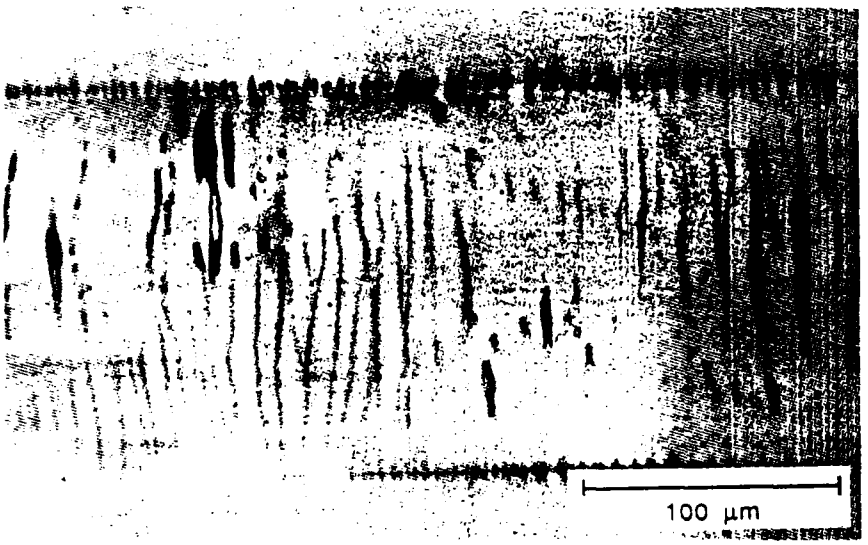

(b)

Fig. 6. a) Thin section transmitted light optical micrograph of as-grown $AgGaSe_2$ showing linear defects having rod-like fine structure.
b) Thin section transmitted light optical micrograph using IR-sensitive film showing similar types of scattering defects.

Fig. 7. Strain fields surrounding analogous defects in as-grown $AgGaSe_2$.

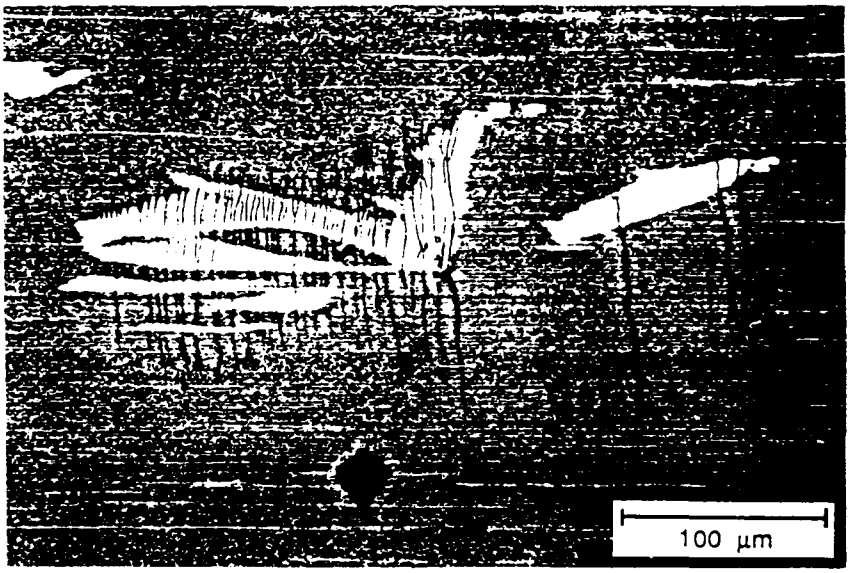

Fig. 8. Reflected light optical micrograph of ion beam milled as-grown $AgGaSe_2$ specimen reveals plate-like morphology of precipitates.

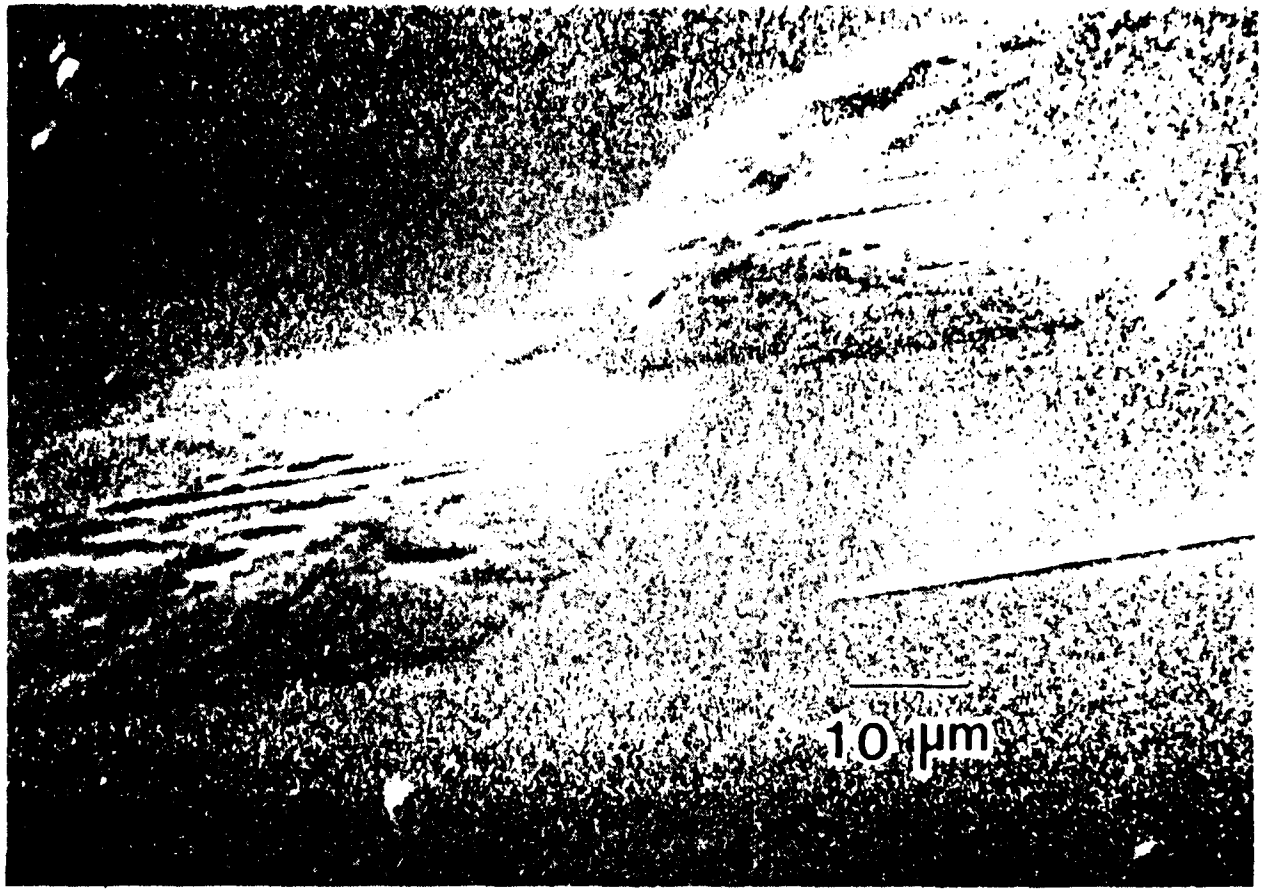

Fig. 9. Well defined plate-like morphology and rod-like fine structure revealed in $AgGaS_2$ by ion-beam milling.

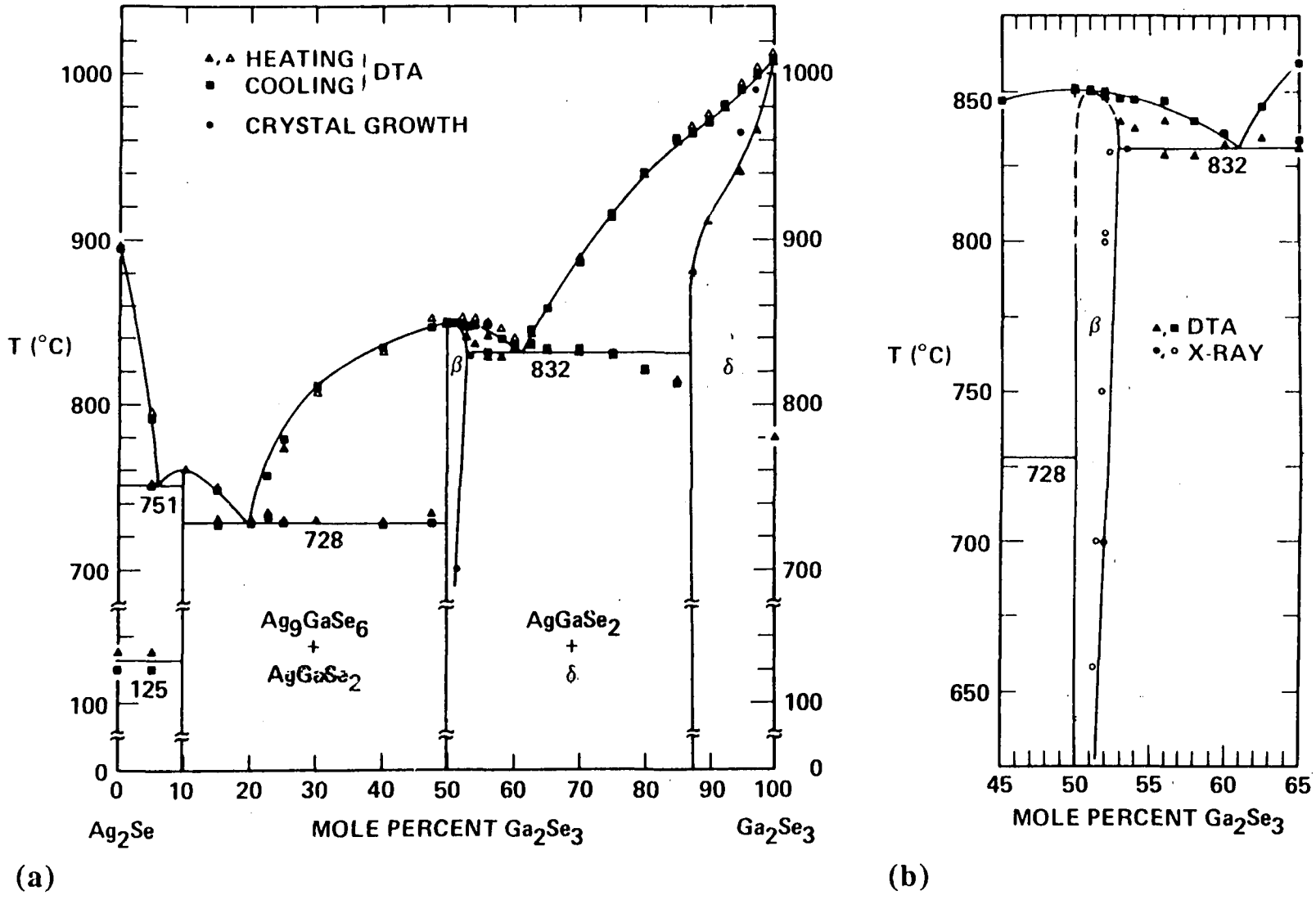

Fig. 10. a) Phase equilibria in the Ag_2Se-Ga_2Se_3 pseudobinary system after Mikkelsen.[14]
b) Proposed modification showing the maximum liquidus temperature at a slightly Ga_2Se_3-rich composition.

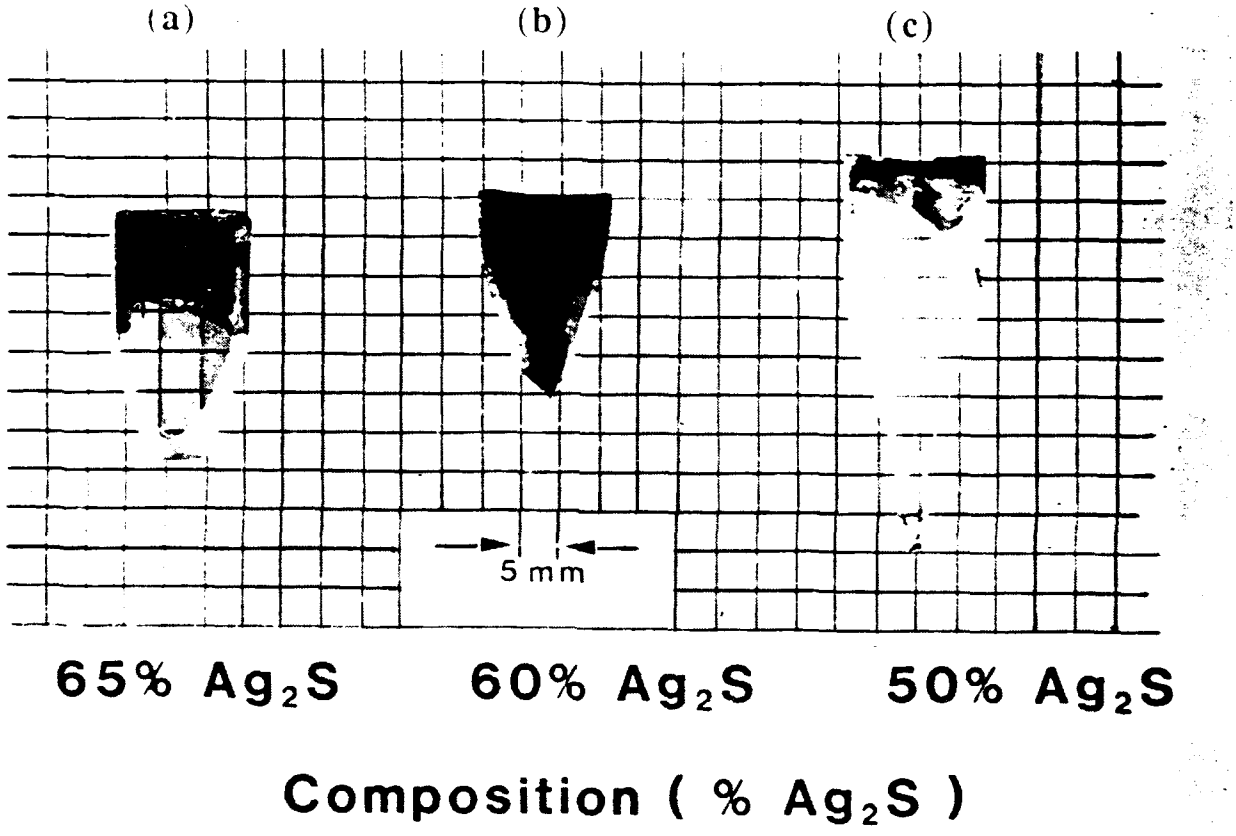

Fig. 11. $AgGaS_2$ crystals grown from solutions rich in Ag_2S.
a) Free of scattering defects from a solution of 65 mole % Ag_2S and 35 mole % Ga_2S_3,
b) with scattering defects from a solution of 60 mole % Ag_2S and 40 mole % Ga_2S_3,
c) with scattering defects from a solution of 50 mole % Ag_2S and 50 mole % Ga_2S_3.

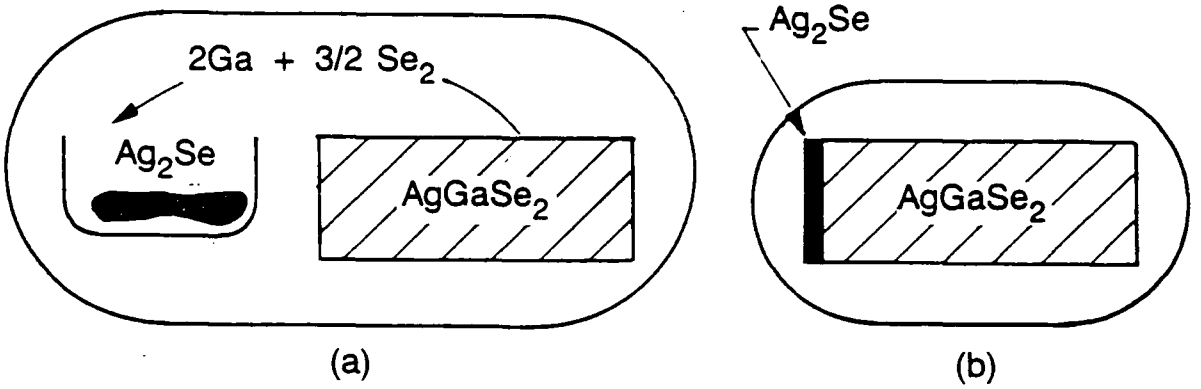

Fig. 12. Postgrowth heat treatment method used to eliminate optical scattering defects from $AgGaSe_2$ crystals at 800° C over a 14-21 day period.
a) No direct contact.
b) Direct contact.

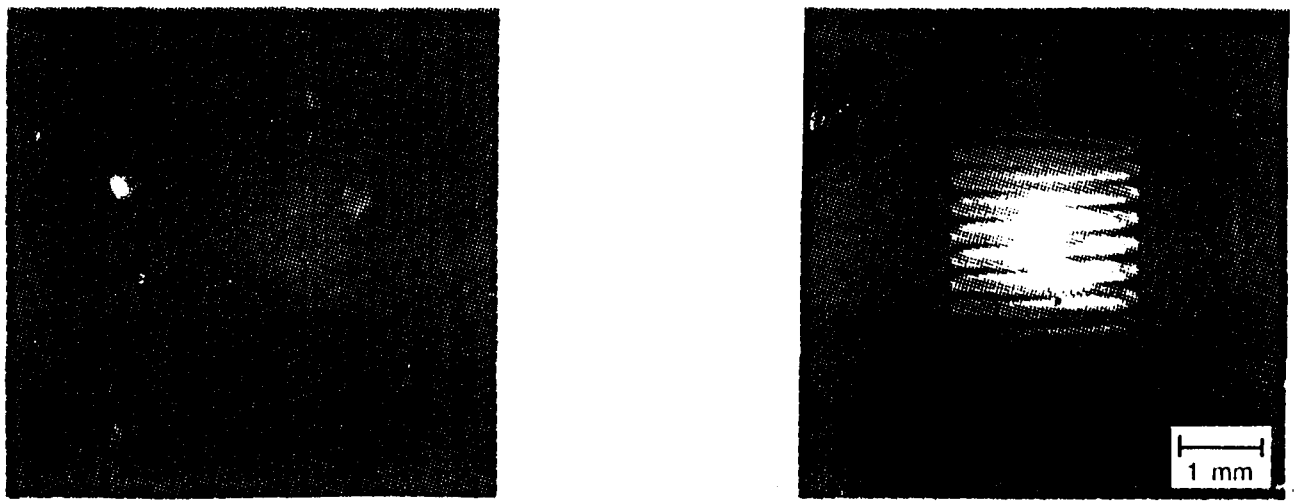

(a) (b)

Fig. 13. Tungsten filament imaged through a 1 cm crystal of $AgGaSe_2$ using IR image converter,
a) a crystal as-grown from a stoichiometric melt, and
b) a crystal after heat-treatment.

Fig. 14. Internally faceted voids shown by SEM that occasionally remain in varying densities after heat-treatment. Their presence does not appear to influence the optical properties of fabricated crystals.

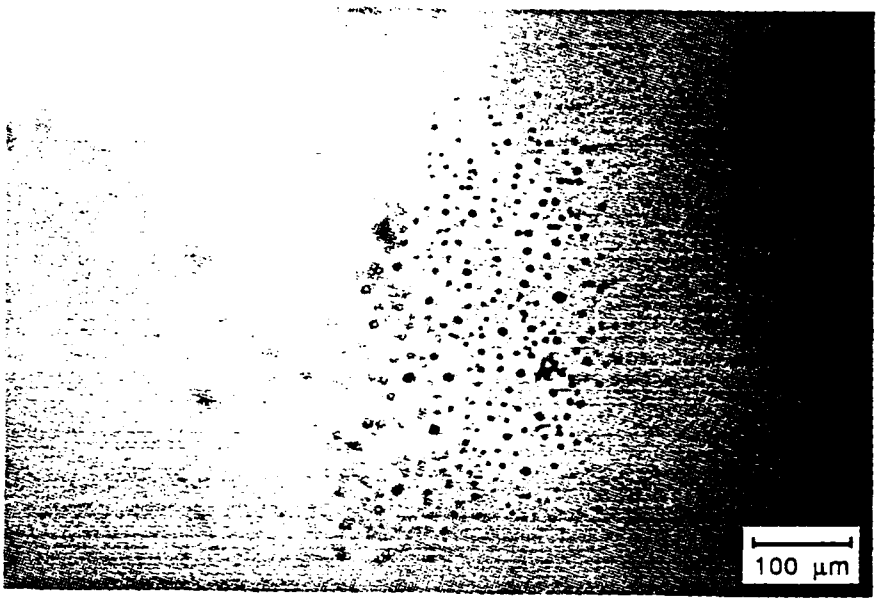

(a)

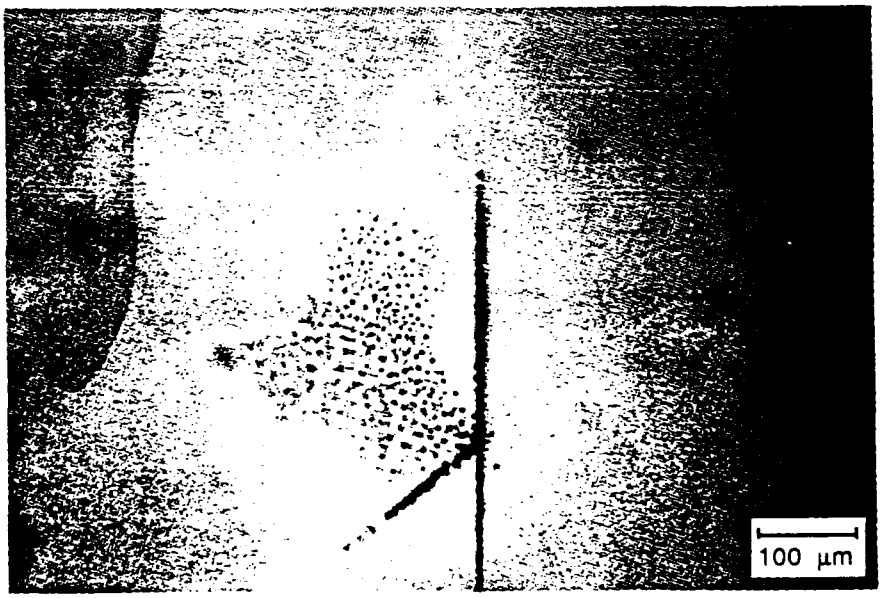

(b)

Fig. 15. Optical micrographs (transmitted visible light) of remnant scattering defects. Three dimensional clusters of
a) random shape, and
b) shapes reminiscent of precipitates in as-grown materials as seen.

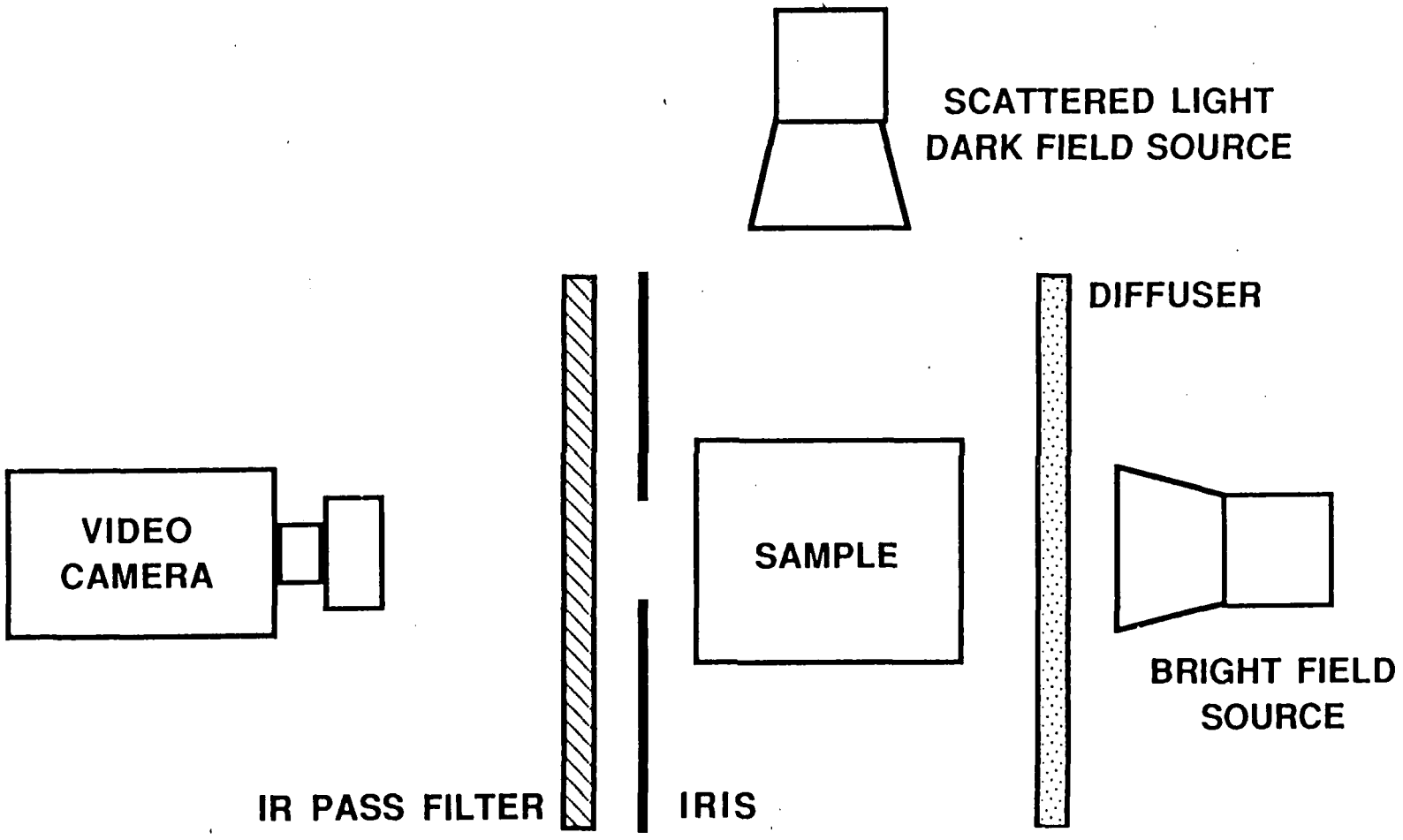

Fig. 16. Video infrared image converter setup which substantially improves our ability to observe scatter in $AgGaSe_2$ crystals.

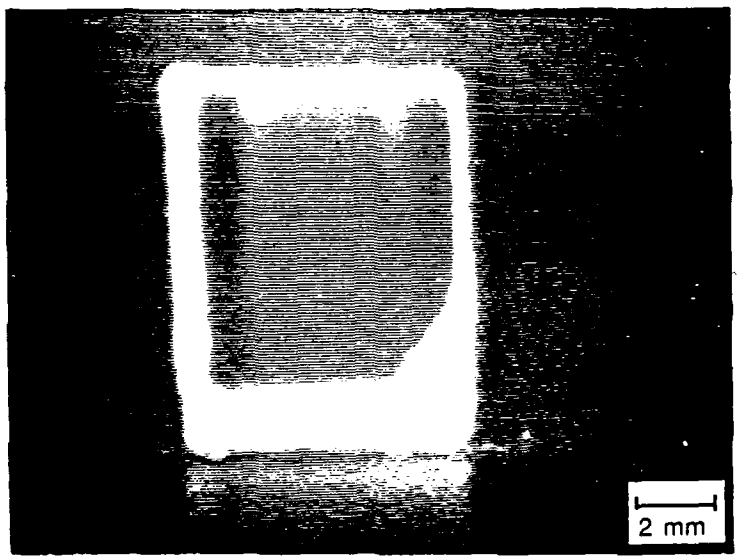

Fig. 17. Video display showing enhanced scattering from a central band (core) and clear bands beneath the surfaces exposed during heat-treatment.

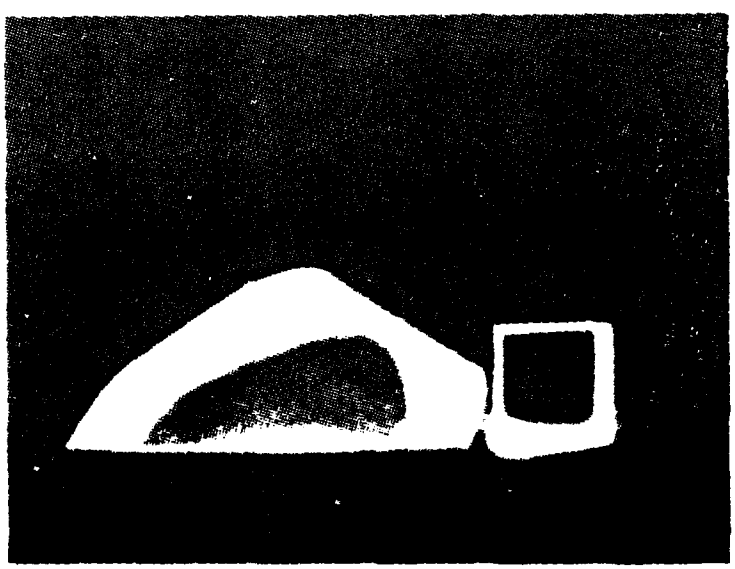

Fig. 18. Dark field scattered light video image of a 1 cm thick singly heat-treated crystal on left, in which weak compositional banding can still be seen, and a 3 cm thick doubly heat-treated crystal on the right, in which no bulk scatter can be seen.

(a)

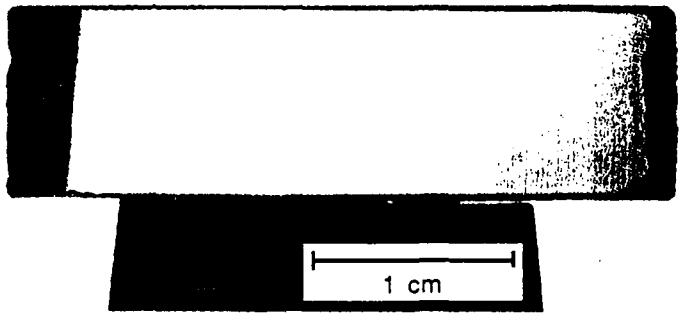

(b)

Fig. 19. Bright-field video display of 1 cm thick $AgGaSe_2$ bars.
a) Singly heat-treated crystal showing a clear boundary between the core region containing scattering defects and the clear region surrounding it.
b) Doubly heat-treated crystal.

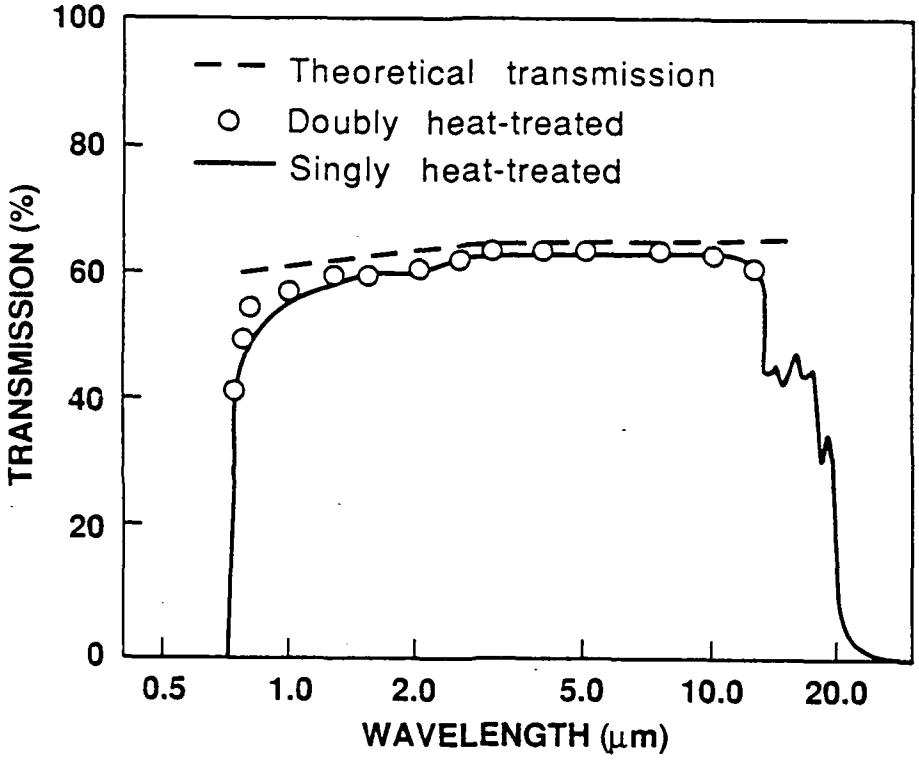

Fig. 20. Spectral transmission of singly and doubly heat-treated $AgGaSe_2$ crystals obtained by conventional dual beam spectraphotometry.

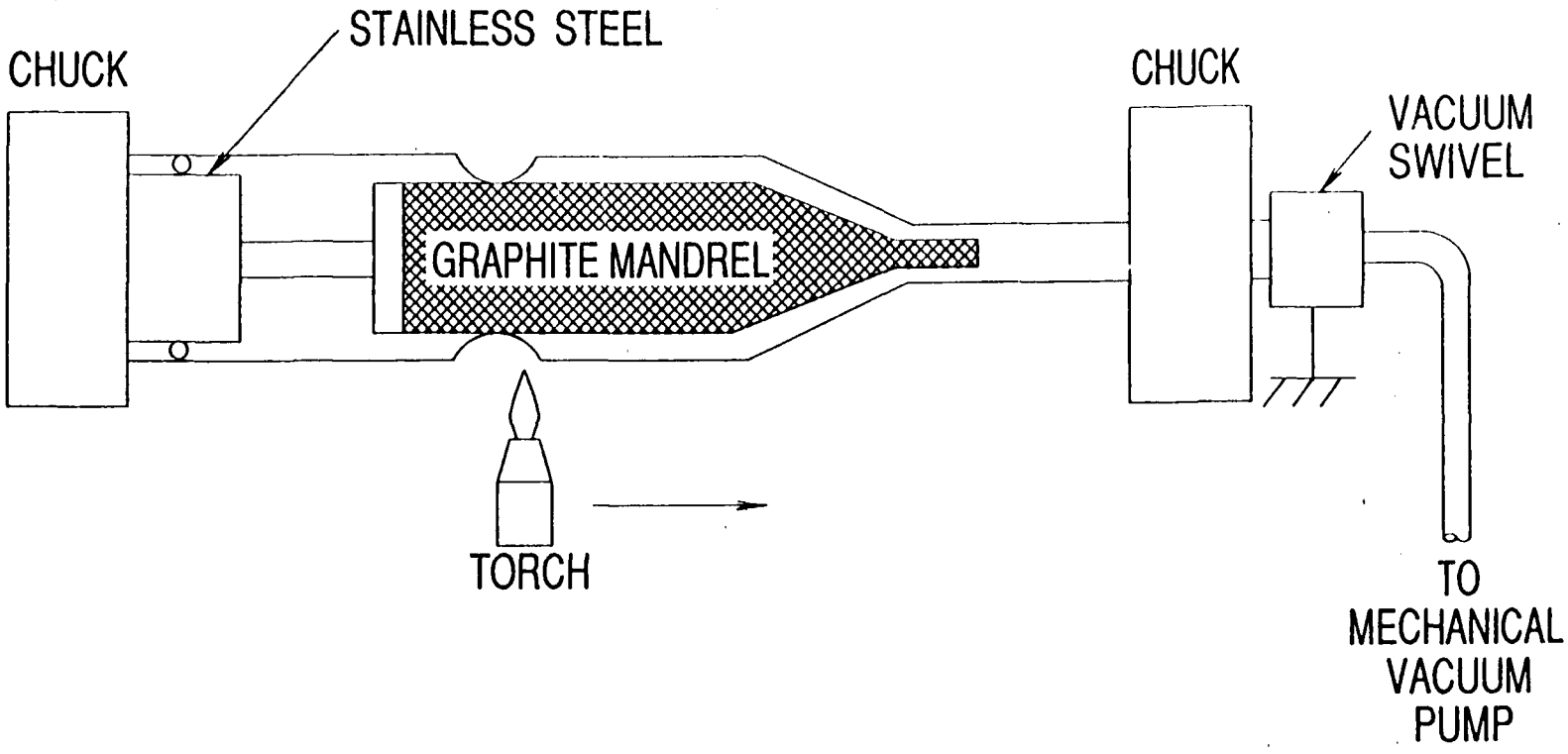

Fig. 21. Vacuum-forming technique used to collapse fused quartz tubing onto precision graphite mandrels.

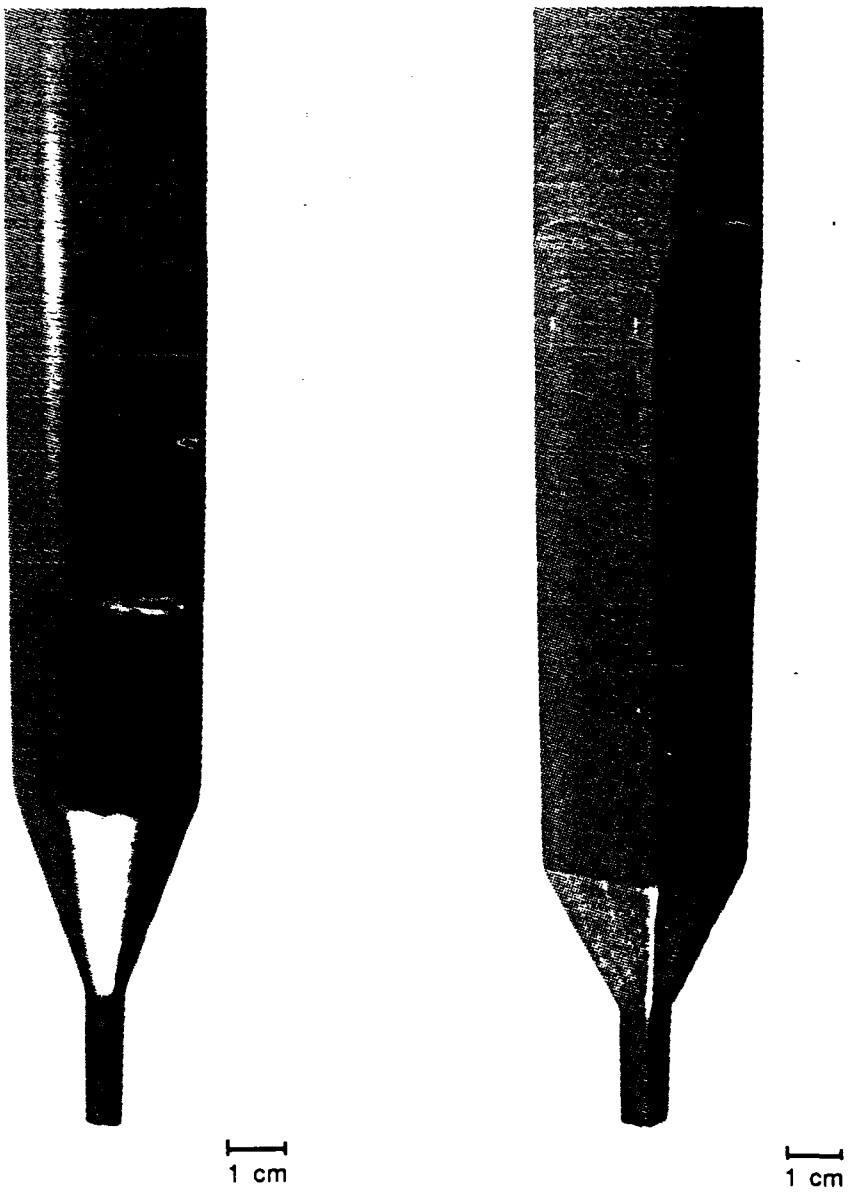

Fig. 22. Precision graphite mandrels with 1 1/2° continuous taper in the bodies. The seed pockets of both circular and square cross-section mandrels are also continuously tapered.

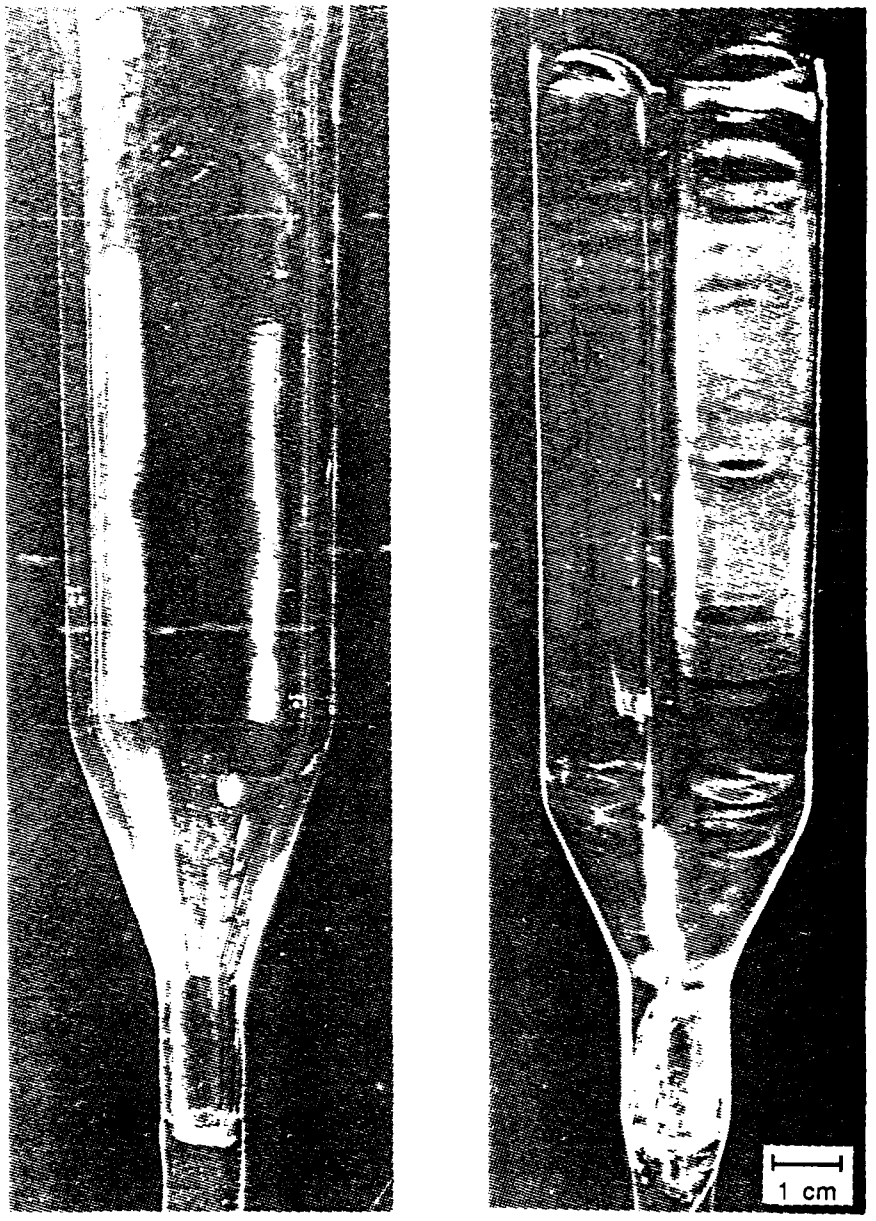

Fig. 23. Vacuum-formed precision tapered fused quartz growth ampoules of
a) 37 mm ID, and
b) 31 mm^2.

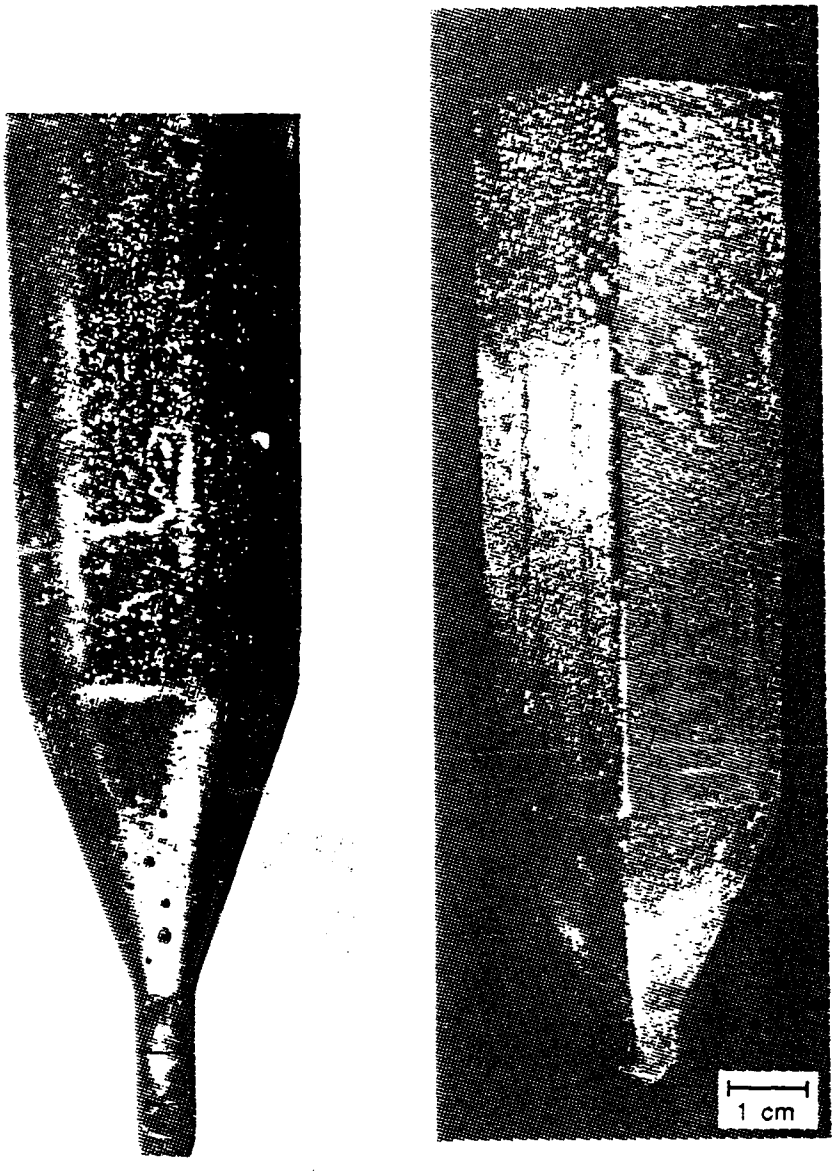

(a) (b)

Fig. 24. As-grown $AgGaSe_2$ crystals in
a) 37 mm diameter, and
b) 31 mm square cross-section.

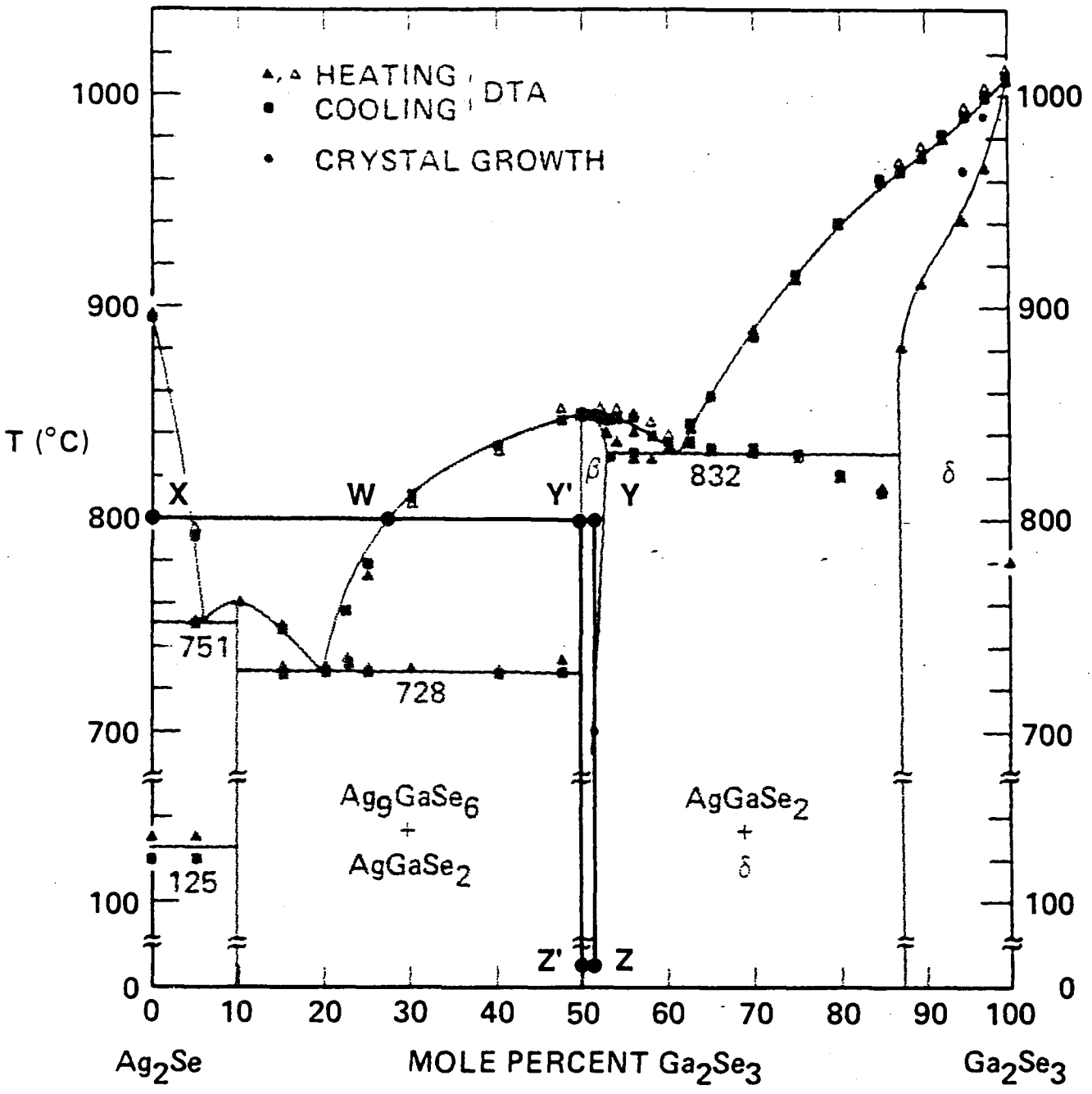

Fig. 25. Phase equilibria in the $AgGaSe_2$ pseudobinary system showing the 800° C diffusion couple (X-Y) used during heat-treatment and the two isoconcentration cooling paths followed by as-grown cloudy crystals (Y-Z) and heat-treated clear crystals (Y'-Z').

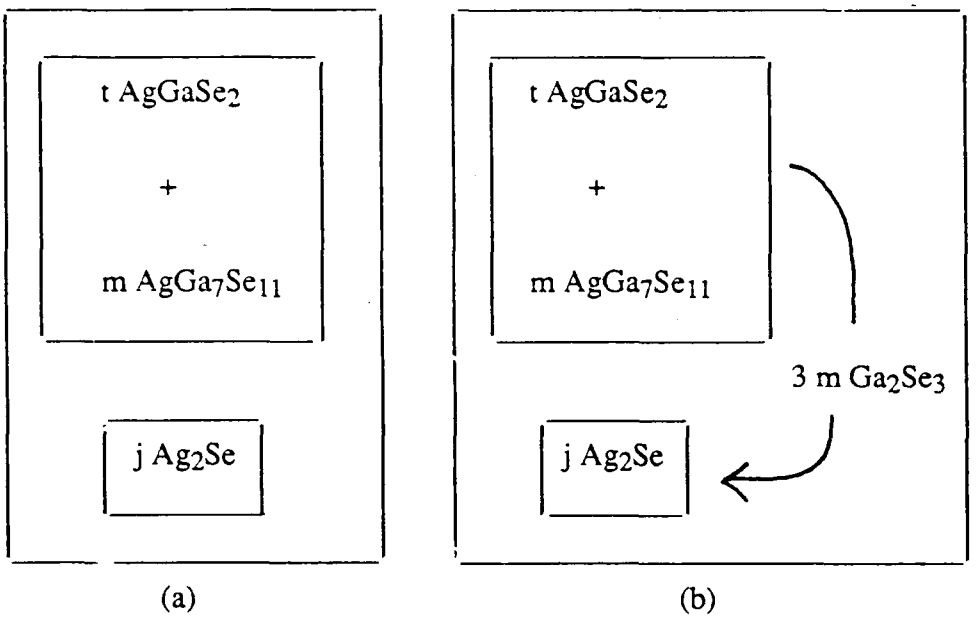

Fig. 26. Schematic diagrams for contactless case:
(a) initial stage, and (b) intermediate stage.

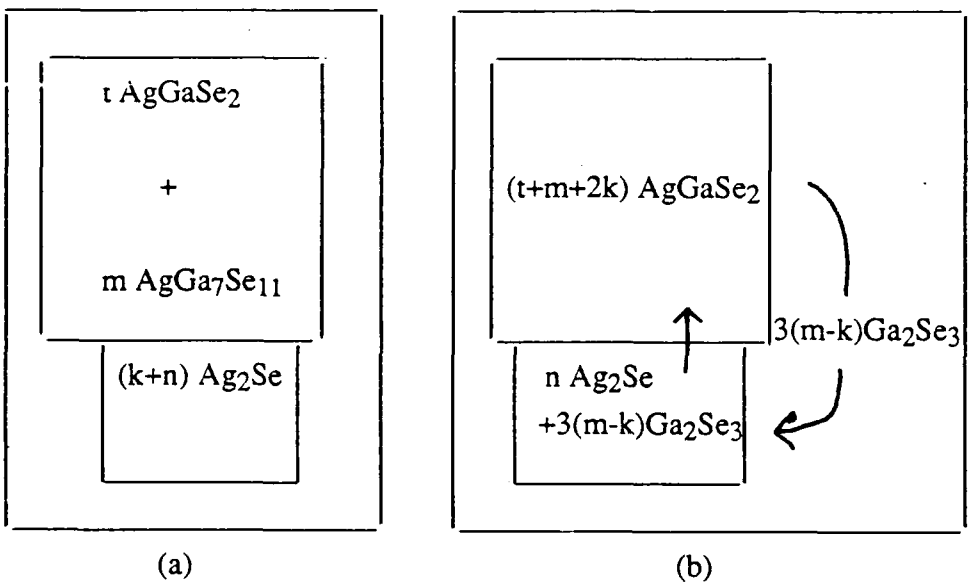

Fig. 27. Schematic diagrams showing the four parameters:
(a) initial stage for contact case, and
(b) final stage for contact case.

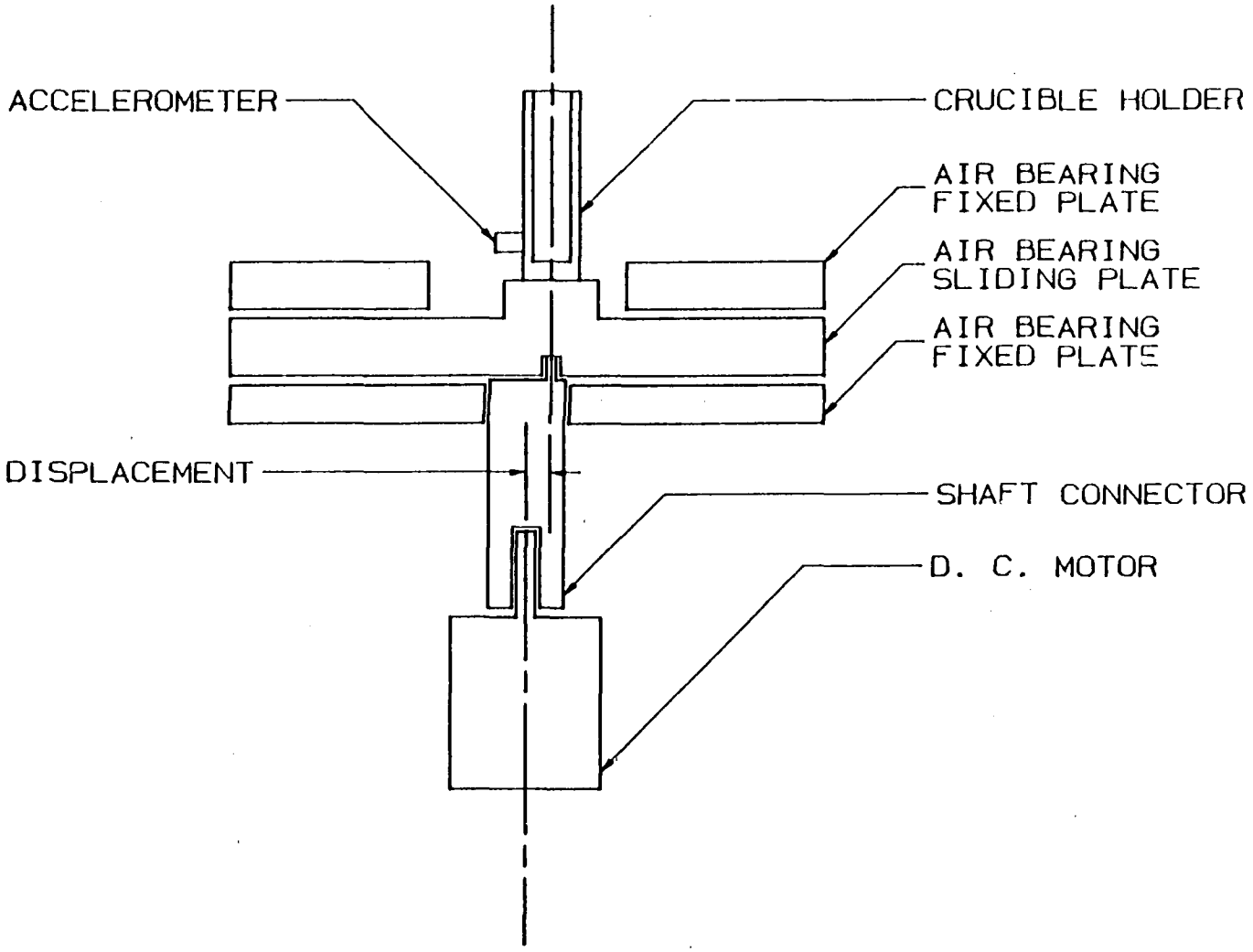

Fig. 28. Coupled vibrational stirring (CVS) apparatus.

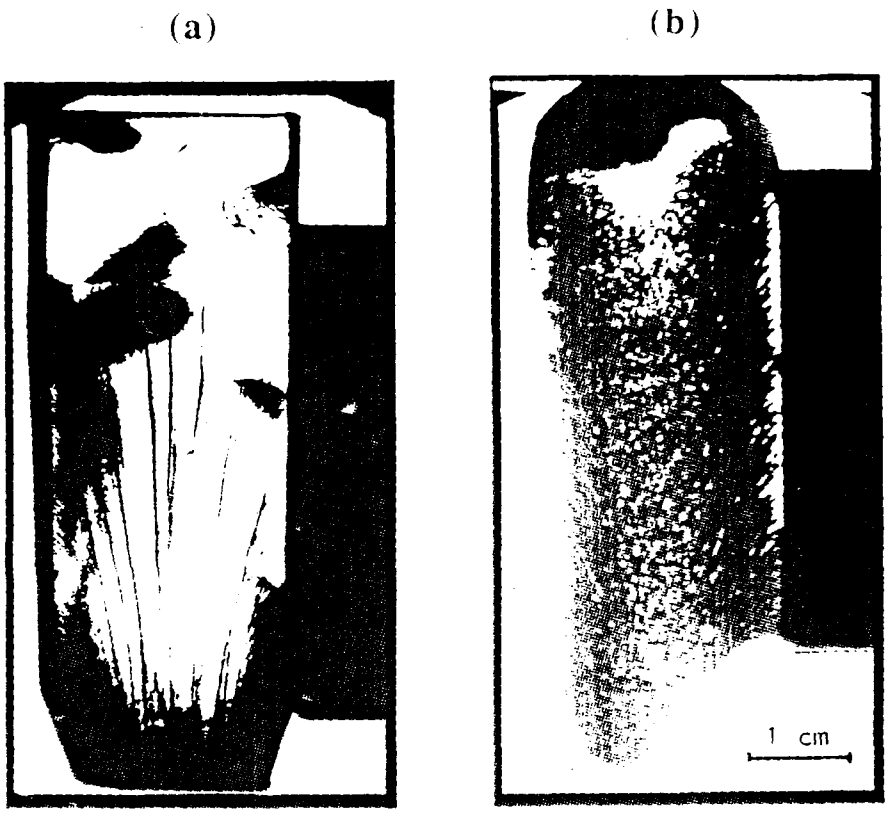

Fig. 29. Bright field transmission video images of 1 cm thick $AgGaSe_2$ crystals grown at 4 x normal growth rate. In a) CPV resulted in a crystal with only a few cell boundaries,and in b) control growth resulted in a totally polycrystalline boule.

VI. LIST OF MANUSCRIPTS AND PUBLICATIONS

1. R. C. Eckardt, R. L. Byer, L. A. Newman and J. Kennedy, "High Average Intensity Nonlinear Infrared Frequency Conversion in $AgGaSe_2$," CLEO, Anaheim, CA (1988) paper WM33.

2. R. S. Feigelson and R. K. Route, Recent Developments in the Growth of Chalcopyrite Crystals for Nonlinear Infrared Applications," *Opt. Eng.* 26 (2), 113 (1987).

3. R. C. Eckardt, Y. X. Fan, M. M. Fejer, W. J. Kozlovsky, C. D. Nabors, R. L. Byer, R. K. Route and R. S. Feigelson, "Recent Developments in Nonlinear Optical Materials," in Laser Spectroscopy VIII: Proc. 8th International Conf., Are, Sweden (June 1987) ed. W. Persson and S. Svanberg, Springer-Verlag, Berlin (1987).

4. R. S. Feigelson, R. J. Raymakers and R. K. route,"Growth of Nonlinear Crystals for Frequency Conversion," to be published in *Progress in Crystal Growth and Characterization* (1989).

5. R. S. Feigelson and R. K. Route, "Improvements in the Optical Quality of $AgGaSe_2$ Crystals," to be published.

6. R. S. Feigelson and R. K. Route, "Improved Yield of Bridgman Grown $AgGaSe_2$ Crystals using Shaped Crucibles," to be published.